Discovery at the Interface of Science and Engineering:

Science Matters!

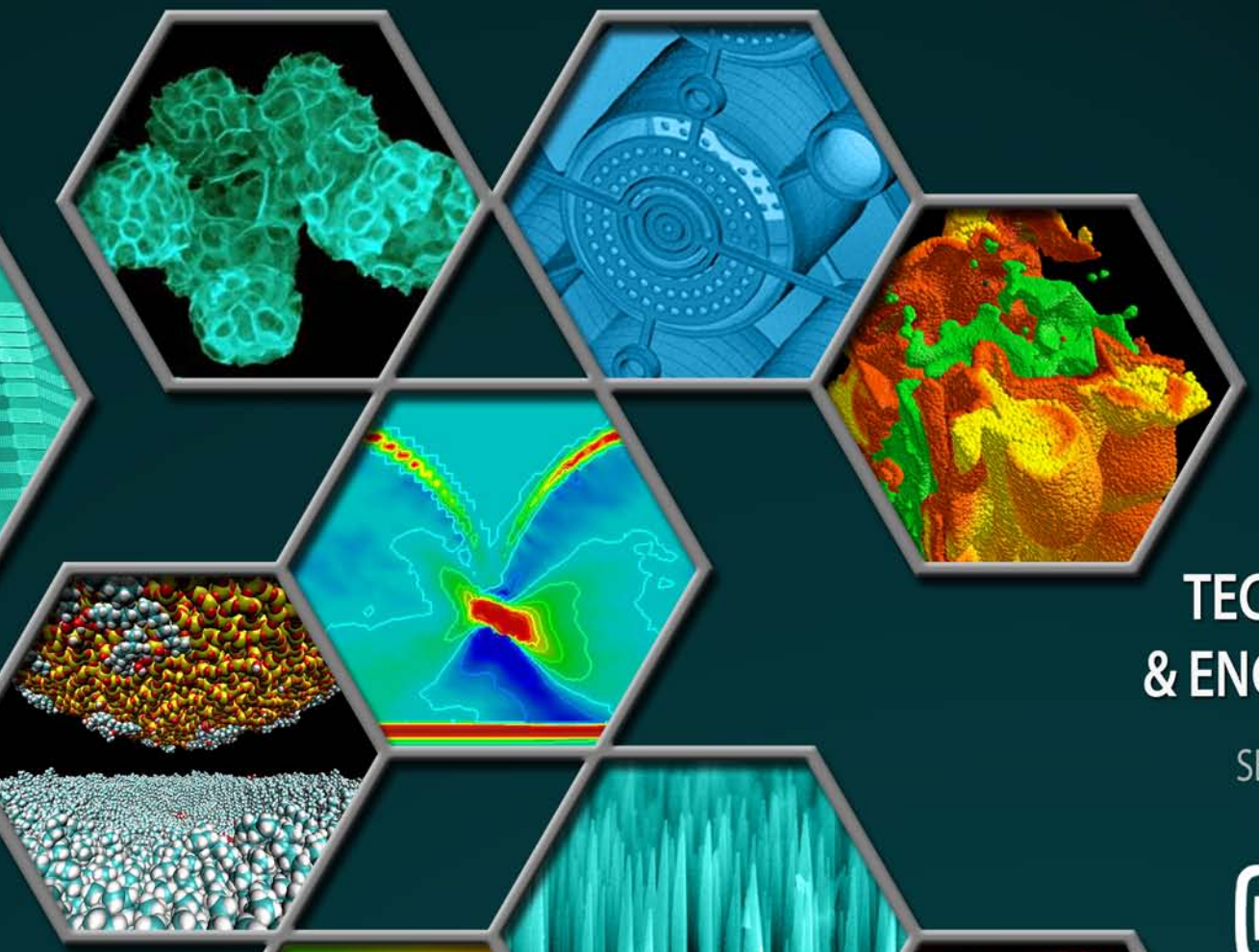

SCIENCE, TECHNOLOGY & ENGINEERING

SEPTEMBER, 2009

Sandia National Laboratories

SAND 2009-5577 P 09/2009
Issued by Sandia National Laboratories, Albuquerque, New Mexico, USA for the US National Nuclear Security Administration (NNSA) Office of Research & Development for National Security Science & Technology, NA-121.

Sandia is a multiprogram laboratory operated by Sandia Corporation, a Lockheed Martin Company, for the United States Department of Energy's National Nuclear Security Administration under contract DE-AC04-94AL85000.

Discovery at the Interface of Science and Engineering: Science Matters!

SANDIA NATIONAL LABORATORIES

Science, Technology and Engineering

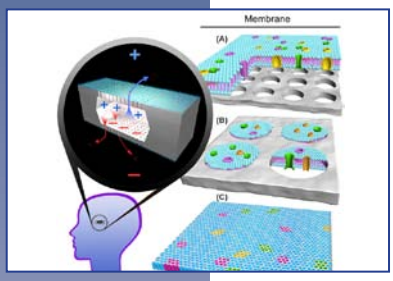

Bioscience

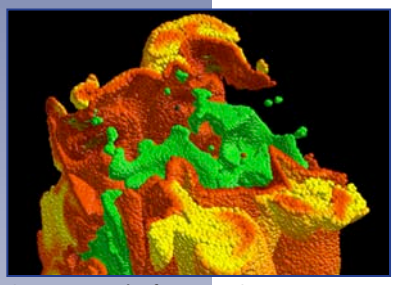
Computers and Information Sciences

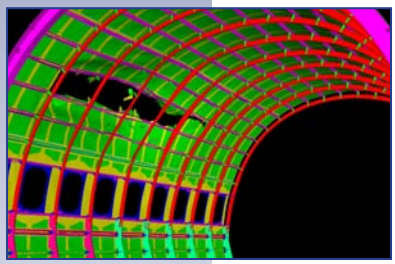
Engineering Sciences

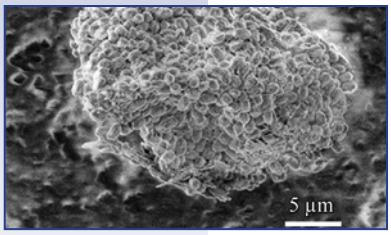

Materials Science and Technology

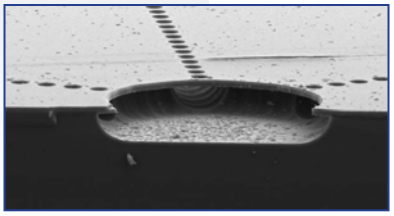
Microelectronics and Microsystems


Pulsed Power

Vision

Sandia National Laboratories is the provider of innovative, science-based, systems-engineering solutions to our Nation's most challenging national security problems.

Mission

Committed to "science with the mission in mind," Sandia creates innovative, science-based, systems-engineering solutions that

- sustain, modernize, and protect our nuclear arsenal,
- prevent the spread of weapons of mass destruction,
- provide new capabilities for national defense,
- defend against terrorism,
- protect our national infrastructures, and
- ensure stable sources of energy and other critical resources.

Guiding principles for ST&E

- Ensure that the fundamental science and engineering core is vibrant and pushing the forefront of knowledge
- Enable the programs by effective application of that science base
  - responding to current needs
  - anticipating the future

About *Science Matters!*

The purpose of ***Science Matters!*** is to publicize and celebrate recent Sandia accomplishments in science, technology, and engineering. We feature the science that underpins and enables technology for Sandia's missions. We nurture expertise, facilities and equipment to create world-class science that pushes the frontiers of knowledge and anticipates future mission needs. New ***Science Matters!*** are being issued semiannually.

Vice President & Chief Technology Officer
J. Stephen Rottler, Ph.D.
505-844-3882
jsrottl@sandia.gov

Deputy, Science & Technology
Charles Barbour, Ph.D.
844-5517
jcbarbo@sandia.gov

***Science Matters!* Point of Contact**
Alan Burns, Ph.D.
505-844-9642
aburns@sandia.gov

Sandia National Laboratories

NNSA National Nuclear Security Administration

Figure Captions *(from top to bottom)*

Biomimetic membranes could form components of useful new nanodevices, such as implantable electrical power sources to drive artificial retina.

A Lagrangian view of autoignition in combustion. Particles in the raw fuel stream are colored by temperature from cold (green) to hot (red).

Simulation results showing tearing in an aircraft fuselage subjected to blast loading. Failure is represented using the "element death" technique.

Scanning electron microscope image of a clump of *B. Anthracis* spores from the anthrax letter sent to Senator Leahy in 2001.

Wet hydrogen fluoride etched buried guidance cues for neural networks on silicon chip. Scale bar = 10 μm.

Lightening caused the 2006 Sago mine disaster in West Virginia.

Contents

Synthetic Biology of Novel Thermophilic Bacteria for Enhanced Production of Ethanol

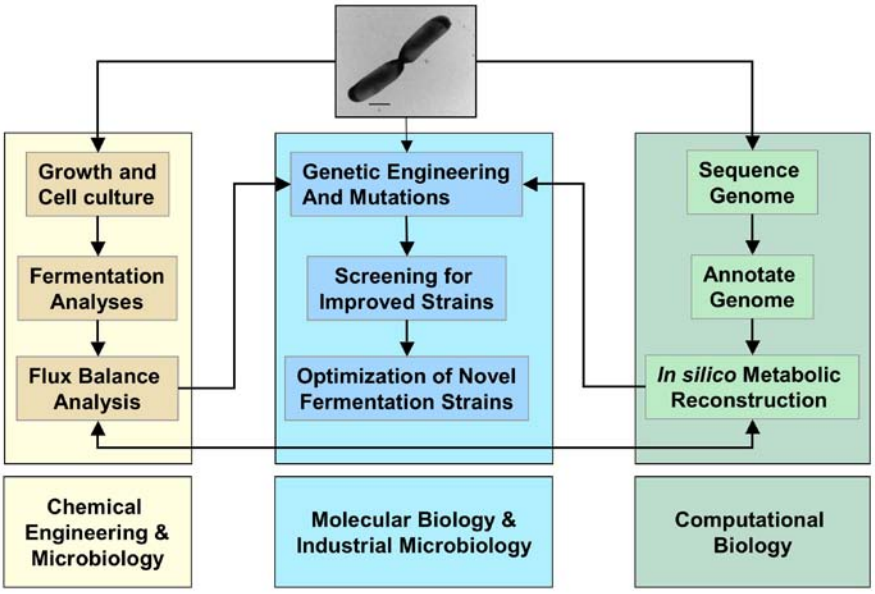

Figure 1: Synthetic Biology is an interdisciplinary approach to design and engineering of biological systems

Sandians are mapping and engineering metabolic pathways for optimum breakdown of cellulose in biomass

For more information:

Technical Contact:
Rajat Sapra
925-294-1580
rapra@sandia.gov

Science Matters Contact:
Alan Burns
505-844-9642
aburns@sandia.gov

Biomass "energy crops" and agricultural waste are preferred long-term solutions for renewable, cheap, and globally-available lignocellulosic feedstocks for biofuels. However, certain technological challenges must be addressed to make the production of biofuels from biomass more efficient and economical in order to replace fossil fuels. The most promising production process (termed SSF for simultaneous saccharification and fermentation) combines the enzymatic hydrolysis of cellulose recovered from biomass to simple sugars, followed by downstream fermentation of the sugars in a single bioreactor. However, SSF is limited in practice because the optimal process conditions for the individual steps differ. Ideally, the SSF process should be carried out at temperatures > 60°C to improve the rate of fuel production, and to decrease byproduct formation resulting in unwanted contamination. This is incompatible with current technologies.

For example, yeasts commonly used for fermentation produce ethanol from C6 sugars (e.g., glucose) at room temperature, and cannot use C5 sugars (e.g., xylose) which form 30-40% of hemicellulosic plant matter. Moreover, industrial enzymatic hydrolysis of cellulose to simpler sugars employs enzymes that have temperature optima of around 55°C, which is much higher than what yeast can tolerate in the downstream fermentation step. Finally, the microbes that utilize both C5 and C6 sugars, unlike yeast, cannot tolerate high ethanol concentrations (>4% by volume). *Geobacillus thermoglucosidasius* M10EXG (*Gth*), a thermophilic bacterium, overcomes some of these limitations. It has an optimal growth temperature of 60°C, can ferment both C5 and C6 sugars, and tolerates ethanol concentrations of up to 10% (by volume), which makes it an ideal microbe to metabolically engineer for improved ethanol production.

Sandia is, therefore, working on improving ethanol production in *Gth* using synthetic biology- a combination of molecular biology, metabolic engineering, computational analysis and microbiology (Figure 1). A basic understanding of the operational pathways is essential to aid engineering; to accomplish that, researchers use metabolic flux analysis (MFA), a high-throughput technology to quantitatively track metabolic pathway activity and determine overall enzymatic function in cells. ^{13}C-labeled glucose and isotopomer flux balance models were used to determine the fluxes through the central metabolic pathways of *Gth* (Figure 2), thus enabling the determination of the theoretical maximum of ethanol production that could be achieved using pathway engineering. Such engineering can be aided by the availability of the genome of an organism; towards that end, Sandia has sequenced *Gth* using a combination of high-throughput pyrosequencing and traditional

Sandia National Laboratories

LDRD LABORATORY DIRECTED RESEARCH & DEVELOPMENT

Sanger sequencing. As currently annotated, the genome of *Gth* is 3.8 Mb (Figure 3), and is shown to contain at least 4300 open reading frames comprising protein coding genes and other accessory genes. Metabolic pathways reconstruction is being currently completed for *Gth*. This interdisciplinary approach is not only useful in engineering native pathways, but also for 'designing' a non-native pathway (Figure 4) that could convert a central metabolite to higher energy density fuel like butanol.

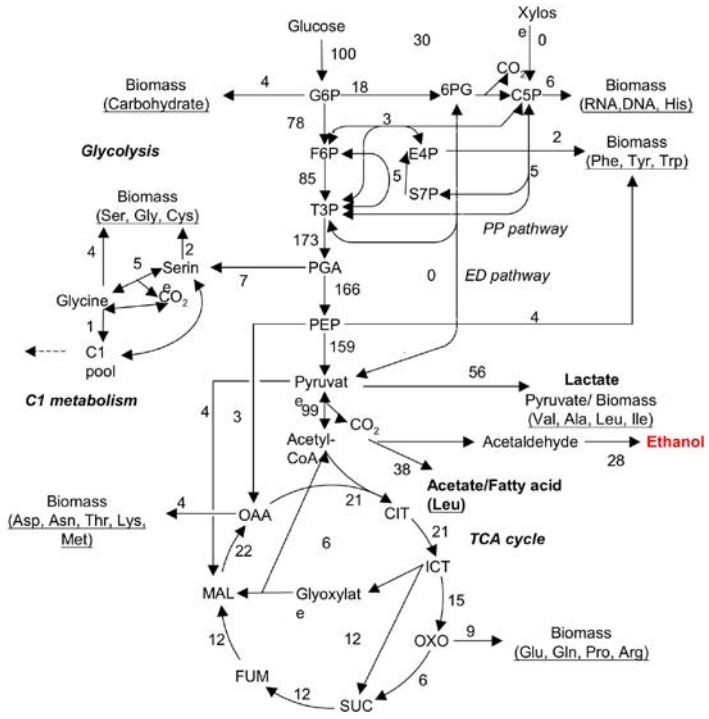

Figure 2: Flux balance analysis of glucose metabolism under micro-aerobic growth of *Gth*.

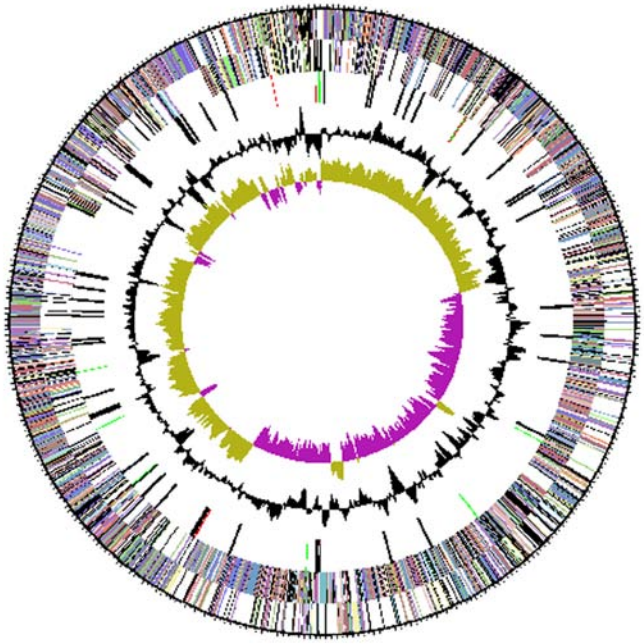

Figure 3: Chromosomal map of *Gth* genes.

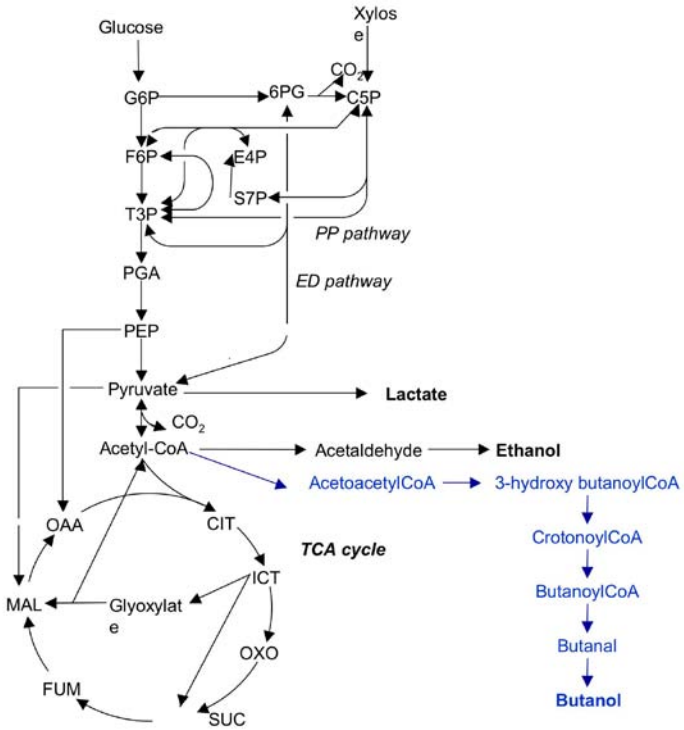

Figure 4: Future direction fuel map: engineering butanol production pathway

Data Discovery from Petascale Combustion Science Simulations

New computational capabilities aide in the development of efficient, clean burning engines and fuels.

For more information:

Technical Contact:
Janine Bennett
925-294-2025
jcbenne@sandia.gov

Jacqueline Chen
925-294-2586
jhchen@sandia.gov

Science Matters Contact:
Alan Burns
505-844-9642
aburns@sandia.gov

Combustion currently provides 85% of our nation's energy needs and will continue to be the predominant source of energy for the near term as the world transitions away from fossil fuels. Transportation is the second largest consumer of energy in the US and there are opportunities for improvements in efficiency of 25-50% through strategic technical investments in fuel and engine concepts and devices. High efficiency low-temperature engine concepts of the future operate in regimes where combustion is poorly understood, and experimentation provides only partial information. Thus, high performance computer simulation at the petascale (10^{15} operations/sec) provides the potential to revolutionize the way we optimize the design of future efficient, clean burning devices that make use of diverse future fuel sources and new combustion concepts.

Over the past several years, through sponsorship from the U.S. Department of Energy, Office of Basic Energy Sciences, Division of Chemical Sciences, Geosciences, and Biosciences and the Office of Advanced Scientific Computing Research, scientists at Sandia's Combustion Research Facility (CRF) have performed and archived a library of direct numerical simulation (DNS) configurations and parametric studies addressing fundamental 'turbulence-chemistry' topics. These terascale (10^{12} operations/sec) studies, enabled by compute time granted under the Innovative and Novel Computational Impact on Theory and Experiment Program, have resulted in a profusion of high-dimensional, complex data. Figure 1 is a multi-variate volume visualization made possible through collaboration with the DOE SciDAC Ultrascale Visualization Institute that demonstrates a recent simulation of a lifted ethylene jet flame, consisting of 1.28 billion grid points and 22 chemical species that resulted in O(300) terabytes being written to disk [Reference 1]. Traditional analysis and visualization algorithms do not extend to inputs of this size, making it challenging to identify, classify, and track complex intermittent features in the resulting data.

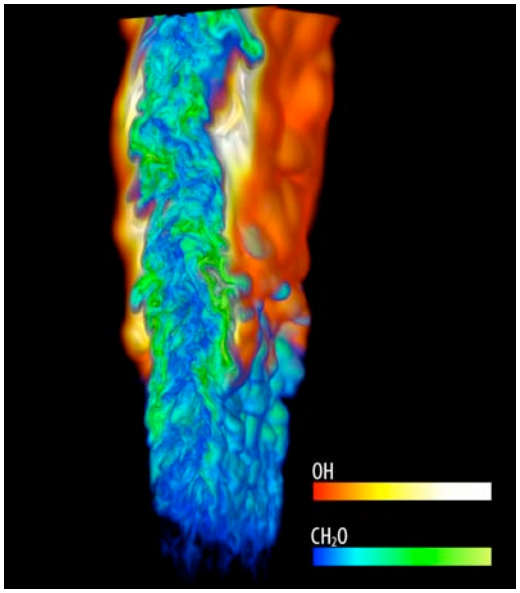

Figure 1: DNS of a lifted ethylene/air jet flame at Reynolds Number 10000. The hydroxyl radical (red/white) denotes the lifted flame whereas formaldehyde (blue/green) denotes ignition intermediates upstream of the lifted flame. Volume rendering courtesy of Hongfeng Yu of Sandia.

Towards this end, scientists at the CRF are developing a suite of tools that aide the exploration of DNS data. For example, COMPARED (Combined particle analysis, reduction, exploration, and display) [Reference 2] is a system for managing and performing categorization of large-scale data in a distributed environment that was used to encapsulate the Lagrangian view of autoignition shown in Figure 2. Scalar data is studied using tools from combinatorial topology such as the merge tree, which can be used to identify isovalues of interest on

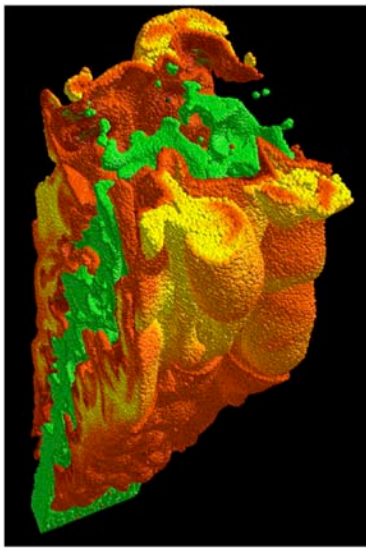

Figure 2: A Lagrangian view of autoignition. Particles in the raw fuel stream are colored by temperature from cold (green) to hot (red). The jet is issuing from the bottom left corner and flows towards the top of the figure.

which to segment the data [Reference 3]. Figure 3 illustrates thin 'pancake-like' structures segmented from the scalar dissipation rate field χ that are subjected to compressive strain by the turbulence in the system. Scientists are interested in the morphology of the χ structures and current research efforts include the development of appropriate shape analysis metrics. Topological analysis is also used to study the relationship between scalar fields. Figure 4 corresponds to a DNS of a lifted autoigniting turbulent jet flame in a hot air coflow, used to investigate the physics of lifted flame stabilization in the presence of ignition. Topological analysis confirms that the χ field and the HO_2 ignition kernels, a marker of ignition, overlap with low probability in regions upstream of the lifted flame base.

Efforts are underway to deploy these tools, together with others currently under development, in a unified framework so that metrics of interest can be studied and explored by scientists, providing fundamental insights necessary to address our nation's current energy needs.

References

1. J. C. Oefelein, J. H. Chen, and R. Sankaran 2009, "High-Fidelity Simulations for Clean and Efficient Combustion of Alternative Fuels," SciDAC 2009, Journal of Physics: Conference Series 180 (2009) 012033, doi:10.1088/1742-6596/180/1/012033.
2. "A Parallel Framework for GPU Enhanced Query and Analysis of Lagrangian Particle Data from Combustion Simulations", R.W. Grout, H. Yu, and J.H. Chen, Poster Session, IEEE/ACM Supercomputing (SC'09), 2009, Portland OR, November 14-20, 2009.
3. Topological Feature Extraction for Exploration of Terascale Combustion Data, A. Mascarenhas, R. W. Grout, P.-T. Bremer, E. R. Hawkes, V. Pascucci, J. H. Chen, in Topoinvis '09: Topological Methods in Data Analysis and Visualization, Snowbird, Utah, February 23-24, 2009.

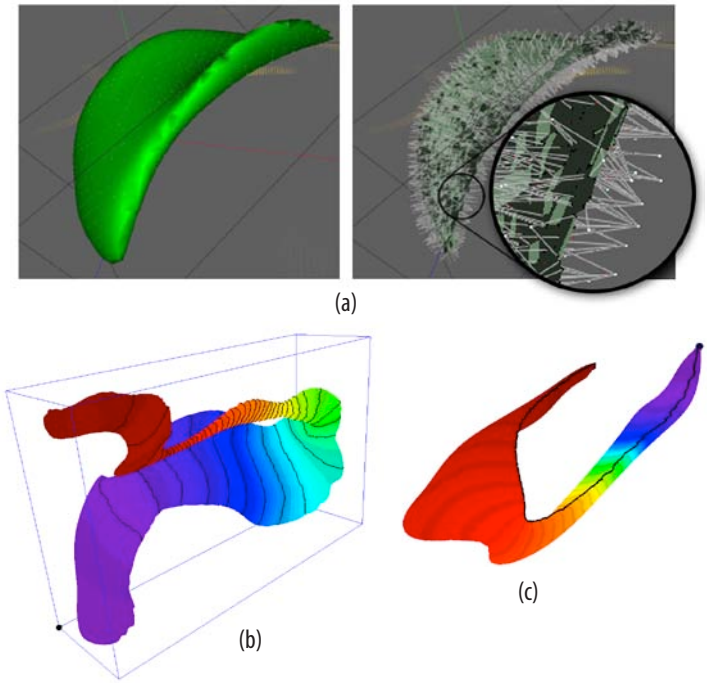

Figure 3: The morphology of the χ structures is studied using several metrics. In (a), the thickness distribution is computed as the distance from the medial axis. In (b) and (c), eigen analysis is performed to obtain circumference distributions and a length measure from the first non-trivial eigen vector of the graph Laplacian of the surface.

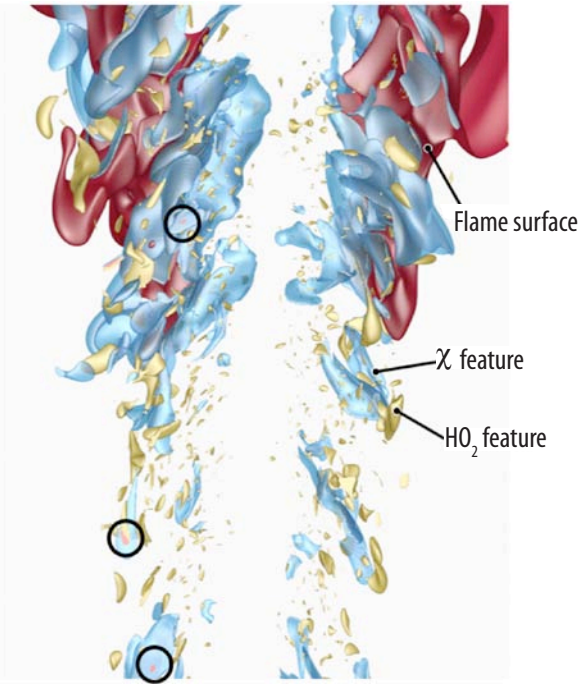

Figure 4: The topological analysis confirms that the χ features (blue) and HO_2 ignition kernels (yellow) overlap with very low probability in the region upstream of the lifted flame base (red). Those regions that overlap greater than a particular threshold have been circled.

Computer and Information Science
Complex systems

Modeling and Simulation of Latent Tuberculosis

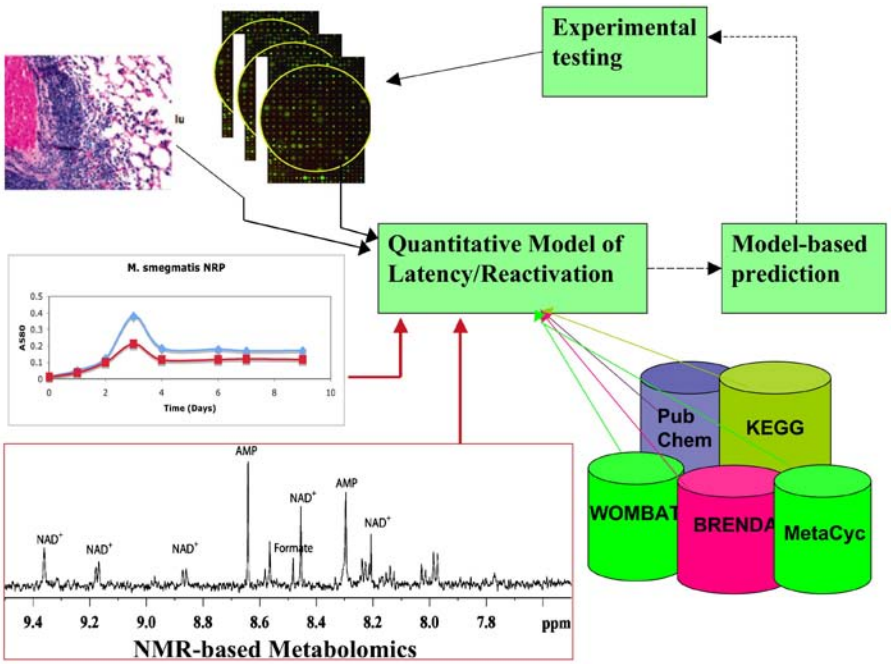

Figure 1: In order to develop predictive, multiscale models of host-Mtb interactions during disease and subsequent latency/reactivation, scientists are integrating quantitative, multi-type immunopathogenesis data (e.g., genomic, metabolomic, and pathogen growth dynamics during latency) with public bioinformatics data resources (e.g., MetaCyc and KEGG warehouse information on biochemical pathways, BRENDA is an enzyme kinetics repository, and PubChem and WOMBAT are useful for obtaining chemical informatics data). The nuclear magnetic resonance (NMR)-based metabolomic data was obtained by T. Alam at Sandia.

Circuit-based framework is used to predict the response of the tubercle bacilli to hostile environmental conditions

For more information:

Technical Contact:
Elebeoba E. May
505-844-9933
eemay@sandia.gov

Science Matters Contact:
Alan Burns
505-844-9642
aburns@sandia.gov

According to the 2008 World Health Organization's report, tuberculosis (TB), caused by the bacterium *Mycobacterium tuberculosis* (Mtb), continues to be a major international cause of illness and death worldwide. Mtb is able to persist in host tissues in a non-replicating persistent (NRP) or latent state. During latency, Mtb is present in the host, but does not produce any overt symptoms; this presents a challenge in the treatment of latent TB. With an estimated one third of the world's population carrying latent TB, reactivation of this highly contagious disease is of great concern, particularly in individuals with weakened immune systems. With nearly four thousand genes and over nine hundred reactions in its reconstructed metabolic network, the identification of which combination of genes and biochemical pathways constitute the "Achilles Heel" of Mtb is a non-trivial task. By coupling advances in high-throughput transcriptomics and metabolimics with large-scale computing, simulation, analysis, and optimization tools, scientists are meeting this challenge. As in other science and engineering fields, modeling and simulation is serving as a transformative bridge in understanding the multiscale phenomena of latency and reactivation in tuberculosis.

Through a five-year grant award from the National Institutes of Health, researchers at Sandia are partnering with the University of New Mexico and Los Alamos National Laboratory to develop models that enable a quantitative understanding of the genetic basis of latency and reactivation in a murine model of tuberculosis. The larger goal of this collaborative effort is to leverage the large-scale biological network simulator BioXyce, based on Sandia's parallel electronic circuit simulation tool Xyce™, to understand the response of Mtb within the microenvironment of a granuloma, which is an aggregation of host immune cells that function to cooperatively quarantine but not completely eliminate the mycobacterium.

Sandia National Laboratories

LDRD LABORATORY DIRECTED RESEARCH & DEVELOPMENT

Understanding the genetic and biochemical mechanisms Mtb employs to persist within the hostile environment of the granuloma will help identify viable chemotherapies to treat the extremely large number of individuals with latent tuberculosis.

Using the Wayne model of hypoxic (oxygen poor) NRP, scientists are generating multi-scale, high time resolution dynamic profiles of the system in order to produce a high fidelity, predictive quantitative model of Mtb response to varying environmental conditions (Figure 1). *In vitro* studies of Mtb in a hypoxic microenvironment suggest that the tubercle bacilli can circumvent the shortage of oxygen by developing alternative energy generation mechanisms by way of the glyoxylate bypass pathway (Figure 2). BioXyce models of this important pathway have been constructed and simulations in the absence and presence of various inhibitory molecules have been conducted (Figure 2). Rather than probing the singular effect of a small molecule on a target protein, a large-scale circuit simulation framework enables researchers to probe in parallel the ripple effect a single molecule or group of small-molecules has on the entire system. This approach, coined "systems chemical biology", is being used to identify small molecules that directly or indirectly interfere with latency-related pathways (Figure 2). As advances in biotechnology propel science deeper into the "omics" age, large-scale simulation is quickly becoming the enabling link that transforms biological data into scientific discoveries in the medical, environmental, and energy sciences.

References

1. E. May, A. Leitao, J-L. Faulon, J. Joo, M. Misra, T. Oprea. Understanding virulence mechanisms in M. tuberculosis infection via a circuit-based simulation framework. IEEE Engineering in Medicine and Biology Society International Conference. 2008.
2. E. May, R. Schiek, BioXyce: An engineering platform for the study of cellular systems. *IET Systems Biology Journal*, **3**(2):77-89, March 2009.

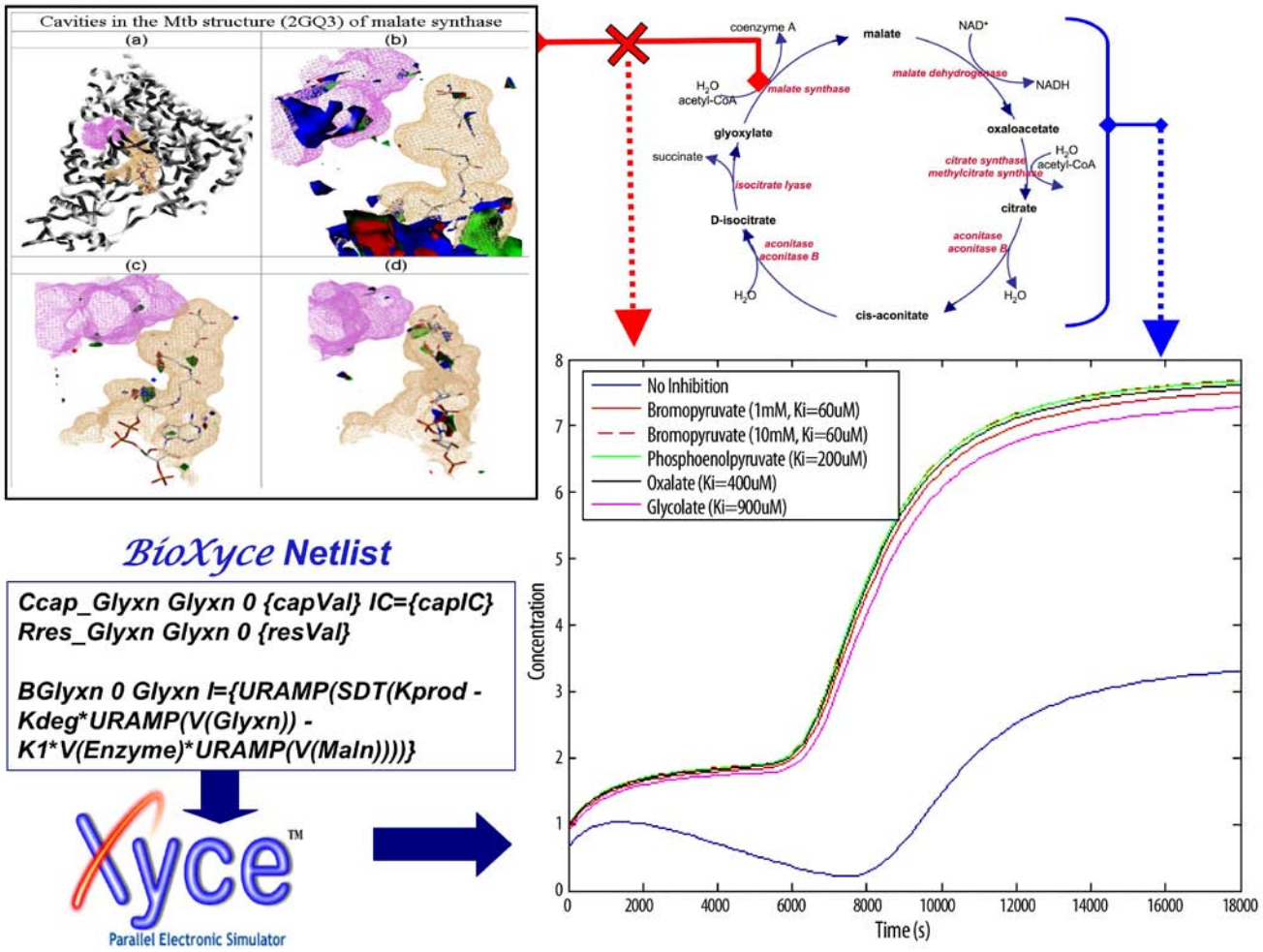

Figure 2: Simulation of the glyoxylate pathway in the presence and absence of inhibitory molecules (figure of small molecule interaction with malate synthase courtesy of Oprea Lab, UNM-HSC Biocomputing Division; pathway recreated from BioCyc, www.biocyc.org).

Engineering Sciences
Fluid Science

Wetting Dynamics on Structured Surfaces

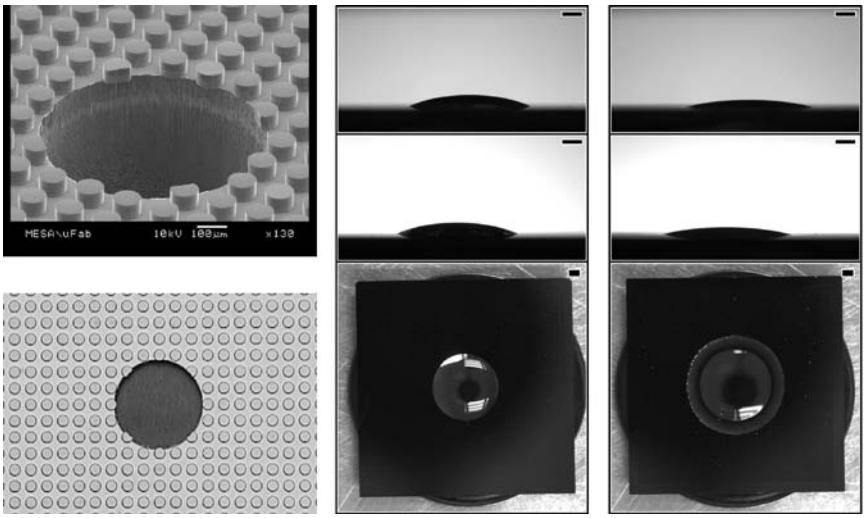

Figure 1: (LEFT) Microfabricated square array of posts 100 µm in diameter with 50 µm minimum gap and a height of 55 µm. Test liquids are pumped through the hole in the center, which is 800 µm in diameter. (MIDDLE and RIGHT) Images of a spreading liquid on plasma cleaned substrates: (MIDDLE) a smooth silicon surface and (RIGHT) the same array of posts shown in the left images. The top two images are profile-views from orthogonal directions; the bottom image is a top-view of the drop. Scale bars are 2 mm. The liquid used is a viscous polymer with low surface tension.

Controlled surface roughness can enhance the spreading of liquids and guide the direction of fluid flows.

For more information:

Technical Contact:
Carlton Brooks
505-284-2454
cfbrook@sandia.gov

Science Matters Contact:
Alan Burns
505-844-9642
aburns@sandia.gov

Wetting, which occurs whenever a drop of liquid makes contact with a solid surface, has been the subject of great scientific and technological interest for the past two centuries (References 1-4). It is important in numerous manufacturing processes, such as mold filling and encapsulation, the application of coatings, and joining (soldering, brazing, and welding). In addition, it is also a critical phenomenon needed for the performance of some devices, such as fuel cells, heat pipes, and the emerging fields of microfluidics and optofluidics.

The structure of surfaces can significantly influence the observed wetting behavior (Reference 5). We have prepared silicon substrates with well-defined microfabricated structures to study how these surface features affect wetting dynamics (Figure 1). Test liquids are pumped through a hole in the substrate and spontaneously spread on the surface. Images of the drop profile from two orthogonal directions and from above are acquired and then analyzed to determine the location where the air-liquid interface intersects the substrate (contact line), the contact angle, and the contact line velocity. In Figure 1, images of a drop spreading on a smooth substrate are compared to a substrate with posts. The post array creates a wicking structure that draws liquid into it using capillary forces. The presence of this thin liquid film advancing ahead of the original drop can be seen as a halo around the main drop, and is not observable with the smooth substrate.

The type of surface texture can also impart dramatically different results. In Figure 2 is a comparison of wetting at different times on a smooth surface, a square array of posts, a square array of vias (microfabricated holes), and a surface with repeated lines/trenches. Compared to posts, the lack of connectedness in the via geometry inhibits the ability of the capillary forces to draw fluid away from the original drop. Liquid penetrating into the vias resists the movement of the contact line and reduces the spreading of the drop. Directional wetting can also be achieved by introducing anisotropy to the roughness using trenches (far right in Figure 2). In this case, the liquid preferentially advances in the direction of the trenches. Bright fringes extending from the leading edges of the drop are due to wicking within the trenches and are observed on the top

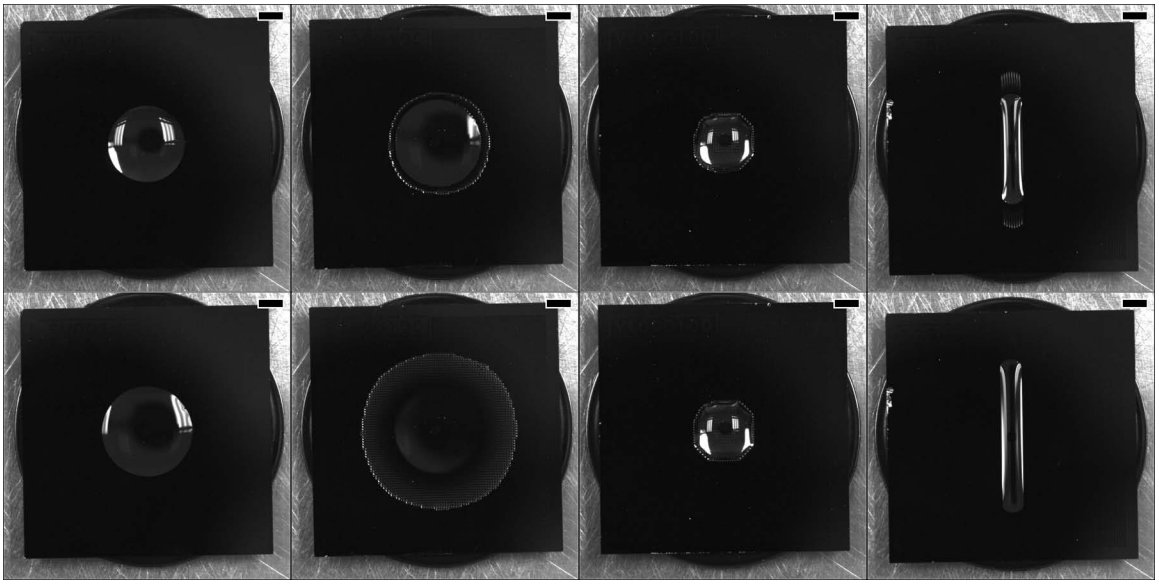

Figure 2: Top view images of a spreading sessile drop on various surfaces (columns). From left to right the substrates are: 100 µm diameter posts arranged on a square array with a 200 µm pitch, 100 µm diameter vias arranged on a square array with a 200 µm pitch, and 100 µm lines with 100 µm trenches. All structured surfaces have a feature height of 55 µm. The time sequence is 30 s (top row), 120 s (bottom row). Scale bar is 2 mm.

and bottom. By changing the trench geometry (Figure 3), quantitative differences in the dynamics can be designed into the substrate. Increasing the trench width at constant pitch results in the main drop spreading faster and lowers contact angle for a given velocity (i.e., reduced resistance to contact line movement).

This work demonstrates that control of surface roughness can be used to enhance the spreading of liquids and guide the direction of multiphase flows. Such control, for example, would be advantageous in encapsulation processes to guide flow and avoid trapped air pocket defects. Directing and timing the propagation of the liquid in combination with the optical properties of interfaces could also be used in a type of optical switch. Since wetting is a broadly applicable phenomenon, numerous applications that leverage the effect of structured surfaces on wetting are possible.

References

1. Young, T. "An Essay on the Cohesion of Fluids," *Philos. Trans. R. Soc.* London 1805, **95**, 65.
2. Fox, H.W., Zisman, W.A. "The Spreading of Liquids on Low Energy Surfaces. I. Polytetrafluoroethylene," *J. Coll. Sci.* 1950, **5**, 514.
3. de Genne, P.G. "Wetting: Statics and Dynamics," *Rev. Mod. Physics* 1985, **57**, 827.
4. Bonn, D., Eggers, J., Indekeu, J., Meunier, J., Rolley, E. "Wetting and Spreading," *Rev. Mod. Physics* 2009, **81**, 739.
5. Quéré, D. "Wetting and Roughness," *Ann. Rev. Mater. Res.* 2008, **38**, 71.

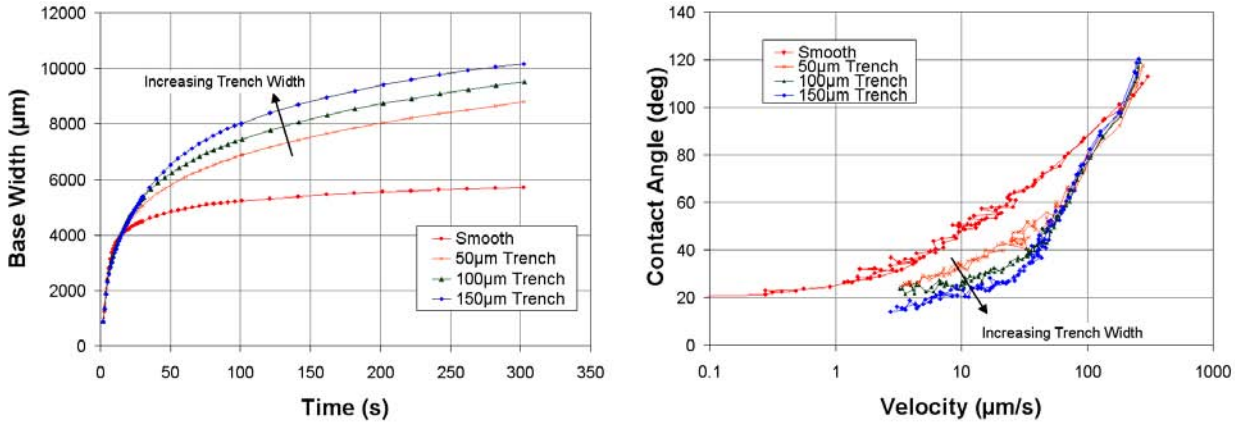

Figure 3: Drop spreading dynamics parallel to the trenches patterned on a silicon wafer. The trench depth is 55 µm and the pitch is kept constant at 200 µm. The liquid used is a viscous polymer with low surface tension. On the left is a time plot of the width of drop making contact with the substrate observable from a profile view (i.e., not the film wicking within the trenches) and on the right is a plot of the dynamic contact angle vs. velocity.

Engineering Sciences
Structural Dynamics

The Science of Material Failure Simulation

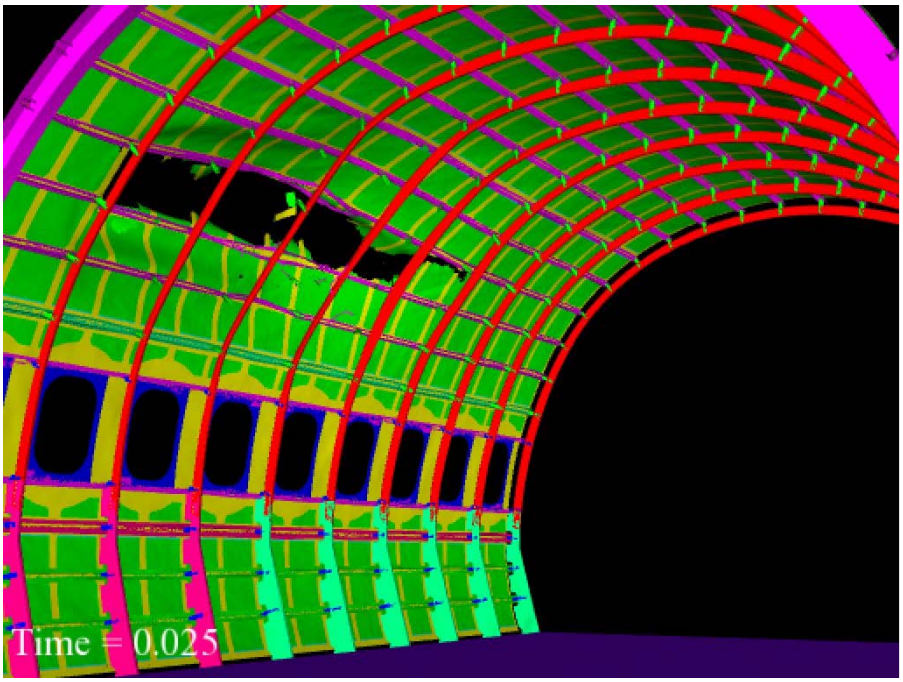

Figure 1: Simulation results showing tearing in an aircraft fuselage subjected to blast loading. Failure is represented using the element death technique.

Predicted behavior of materials under extreme stress is crucial to providing safety and security in weapons systems

For more information:

Technical Contact:
Ben Spencer
505-844-3778
bwspenc@sandia.gov
John Dolbow
505-845-0875
jedolbo@sandia.gov

Science Matters Contact:
Alan Burns
505-844-9642
aburns@sandia.gov

When structural systems are subjected to excessive or extreme loads such as blasts and high-velocity impacts, the process of material failure gives rise to an eventual loss in structural integrity. Computational science provides one of the most efficient means to examine what types of loads structures can sustain, as well as predict the effects of pervasive failure, should that occur.

Material failure is widely recognized as a multi-scale problem, linking the breaking of atomic bonds at the nanoscale to the growth of microscale flaws, to the formation and rapid propagation of cracks and free surfaces at the macroscale. Continuum-based models typically focus on material behavior at the microscale and above, employing phenomenological, constitutive models of the bulk response and failure criteria. The challenge for material failure simulation can thus be posed as: given a structural system consisting of known materials and a set of applied loads, predict the mechanical response including the transition to a highly disconnected state. Simulating the response of an aircraft fuselage to blast loading (Figure 1) is an example of such a challenge.

Numerical methods for this class of problems are typically based on discretizations of nonlinear partial differential equations. Well-known methods for continuum-based simulations of material failure include the finite element method and mesh-free/particle methods, as well as hybrid schemes. Under this broad umbrella, several specialized methods are distinguished by the means by which they describe the evolution of the system geometry as failure surfaces are introduced and evolved. A variety of these methods have been developed in the Presto code, which is part of Sandia's SIERRA Mechanics code suite. This code suite facilitates large-scale simulations and interaction with coupled field phenomena.

Sandia National Laboratories

LDRD LABORATORY DIRECTED RESEARCH & DEVELOPMENT

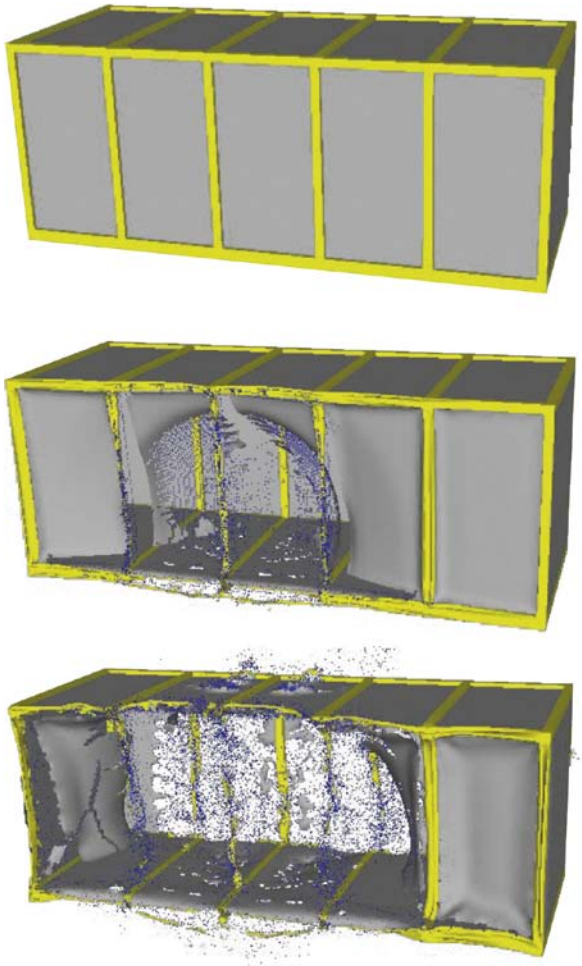

Figure 2: Simulation results of a thin-walled box structure with stiffeners subjected to blast loading showing progression of failure. Failed elements are converted to particles, and contact algorithms are used to prevent penetration of particles into solid material.

With finite element methods, perhaps the simplest technique to represent failure surfaces is known as "element death," wherein elements that are identified as "failed" are simply removed from the simulation. Particle methods often address material failure similarly, by removing communication links between nearby particles in the neighborhood of a failed region of material. For problems in which the contact of debris with intact material is important, failed elements can be converted to particles, as demonstrated in the simulation shown in Figure 2.

Element death techniques suffer from systemic problems such as mesh sensitivity and difficulties identifying unique failure surfaces from the collection of intact elements or particles. To overcome these problems, efforts using SIERRA Mechanics are currently focused on advancing the nodal-based extended finite element method (NBX-FEM). The method explicitly tracks failure surfaces, and enhances element-level kinematics to capture material separation (Figure 3). The bulk material response is carried at the nodes of the finite element mesh, facilitating topology updates when mesh distortion becomes severe.

The techniques discussed in this article will continue to be developed along with multi-length scale techniques that will allow for treatment of material heterogeneity, fine scale processes, and time scale issues. A major technical challenge that is being addressed is the elimination of "mesh" or model size dependence in the failure modeling process. With advancements in these areas, we will be able to predict failure for not only isolated single cracks, but also for problems of pervasive failure such as those associated with fragmentation and the subsequent damage that the fragments will create. This capability will be applied to a wide range of problems in the areas of nuclear weapon safety and security, and also a wide suite of national security problems associated with the Department of Defense.

Figure 3: Deformed geometry for a thick-walled cylinder with a thumbnail-shaped edge crack. The gray elements are enriched with NBX-FEM kinematics.

Diamond-Like Nanocomposites to Mitigate Friction and Wear

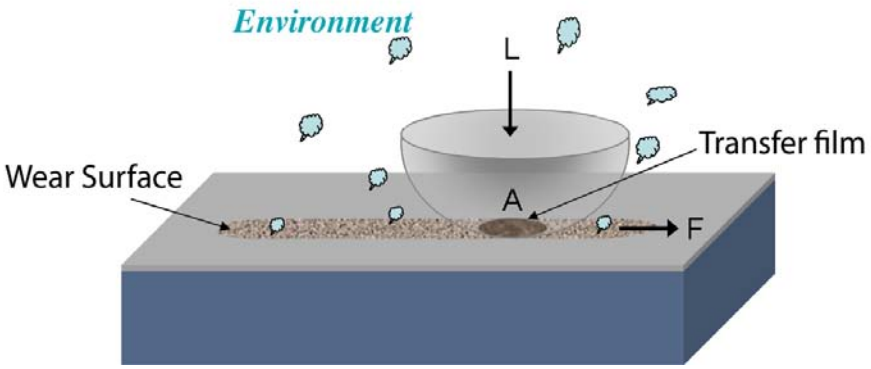

Figure 1: Schematic of a hemi-spherical pin sliding on a coated substrate. Tribology is a systems property, principally governed by tribochemical reactions and contact mechanics.

Many analytical techniques are needed to understand all aspects of friction and wear

For more information:

Technical Contact:
Somuri Prasad
505-844-6966
svprasa@sandia.gov

Science Matters Contact:
Alan Burns
505-844-9642
aburns@sandia.gov

According to the classical theory of Bowden and Tabor, friction force F is a product of the area of contact A and the interfacial shear strength τ (see Figure 1). Thus, the coefficient of friction μ can be expressed by: $\mu = F/L = A\tau/AP = \tau/P$, where P is the contact stress and L is the load. In principle, a hard material with a soft skin ought to provide a low coefficient of friction μ by reducing the interfacial shear τ and increasing the contact stress P. Environment also plays a significant role in determining the tribological behavior of a material. Many tribological contacts result in transfer of material from one surface to the other, plus surface chemical reactions with the surrounding environment, resulting in wear surfaces whose chemistry is significantly different from the bulk.

In the search for an environmentally-robust lubricant between contacting surfaces, Sandia is investigating the fundamental mechanisms of friction in diamond-like carbons, specifically the role of "tribochemistry" on friction. Under consideration is a diamond-like nano-composite (DLN) coating, produced by Bekeart Advanced Coatings Technology, and processed from siloxane precursors by plasma-enhanced chemical vapor deposition. It has an amorphous structure consisting of two interpenetrating networks, a diamond-like (a-C:H) and a quartz-like (a-Si:O), with minimal bonding between the two networks. The DLN coating exhibits environmental robustness with a μ of 0.02 in dry nitrogen and ~0.2 in humid air, with minimal wear in both environments. In both cases, an extremely thin layer of the coating got transferred to the counterface ball during the initial run-in period. In a first-of-its-kind surface analytical study, researchers analyzed the transferred films on the counterface balls by Time-of-Flight Secondary Ion Mass Spectroscopy (ToF-SIMS), and constructed the color montages of SIMS maps (Figure 2) using Sandia's Automated eXpert Spectral Image (AXSIA) software. They believe that by forming transfer films of long range carbon and hydrogenated carbon in dry nitrogen (Figure 2b), and predominantly silicon oxide species in humid air (Figure 2a), DLN is able to adapt itself to both dry and humid environments.

Sandia is also applying focused ion beam microscopy (FIB) and finite element analysis modeling (FEM) to study coating-substrate interface reliability. FIB sections of wear scars are routinely made to visualize friction-induced subsurface deformation and to

validate FEM. In all cases where the contact stress induces plastic deformation in the underlying substrate (see the focused ion beam cross-section of the wear scar on the left in Figure 3), fracture and de-lamination of the coating results. This underscores the need to design the coating architecture (e.g., a hard coating sandwiched between DLN and the softer substrate) to withstand higher operating stresses.

Besides the environmental robustness, there are engineering issues such as coverage on sidewalls, and masking certain areas of a small part to enable subsequent welding and joining operations (Figure 4) that must be addressed. Sandia is currently working on the application of DLN coatings for advanced surety mechanisms to enable designers more flexibility in the choice of the operating environment.

References

1. T. W. Scharf, J. A. Ohlhausen, D. R. Tallant and S. V. Prasad, *J. Appl. Phys.* **101** (2007) 063521.
2. J. M. Jungk, J. R. Michael and S. V. Prasad, *Acta Materialia*, **56** (2008) 1956-1966.

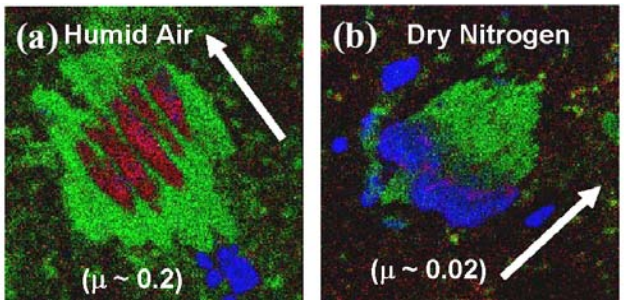

Figure 2: Time-of-flight SIMS (negative secondary ion image) maps of silicon oxide (red), long range carbon (green), and hydrogenated carbon (blue) fragments on the counterfaces generated in (a) humid air and (b) dry nitrogen. The arrow indicates the sliding direction. The image size is 100 x 100 mm^2. Sandia's AXSIA software was used to generate the montage of SIMS image maps.

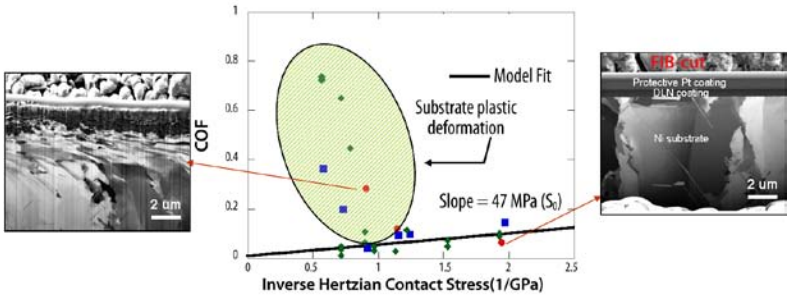

Figure 3: The coefficient of friction (COF)decreases with increasing contact stress, in agreement with the classical theory (straight line). The shaded region corresponds to the case where the contact stress induces plastic deformation in the underlying substrate (see the focused ion beam cross-section of the wear scar on the left), causing fracture and de-lamination.

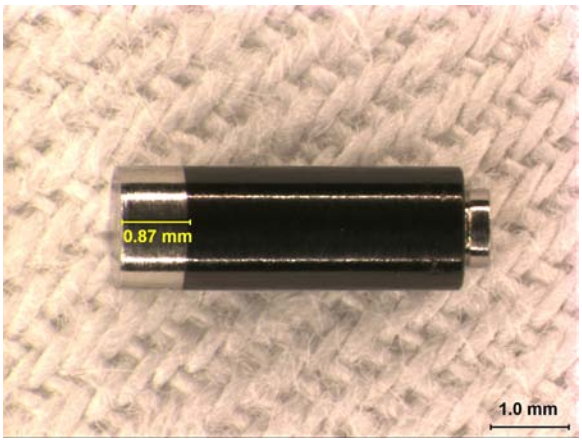

Figure 4: Application of diamond-like nanocomposite coatings for Advanced Surety Mechanism components. One end of the pin was masked to enable subsequent welding and joining operations.

Reliable Mechanical Contacts via Vapor Phase Lubrication

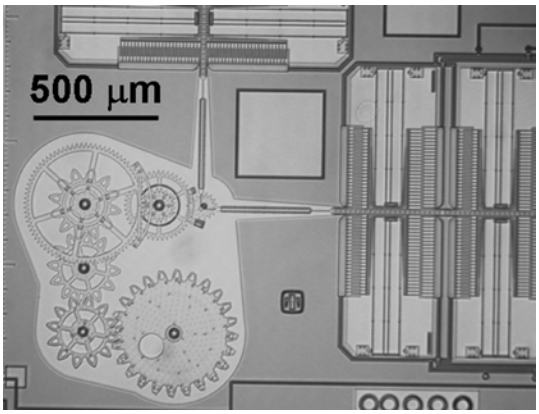

Figure 1: A silicon prototype weapon surety device containing electrostatic actuators (right and top) driving an intermeshing train of six gears.

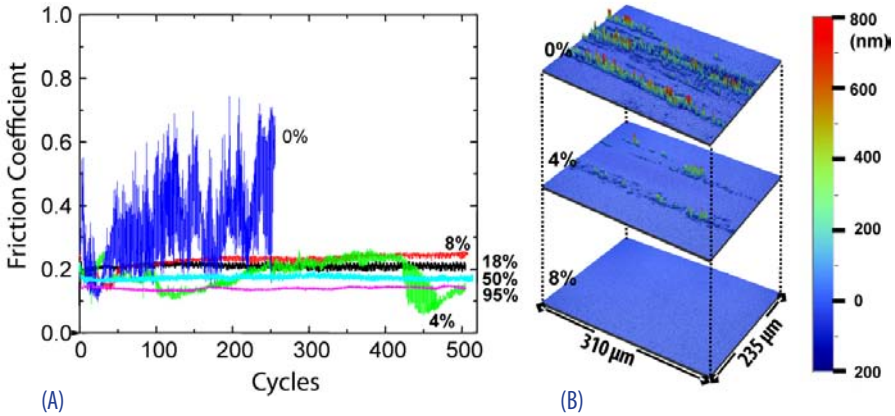

Figure 2: (A) Friction coefficient versus sliding cycles for a silica ball sliding on an oxidized silicon surface in dry N_2 gas (0%) and increasing percentages of the saturation pressure of pentanol. (B) Optical interferometric images of wear tracks for the dry, 4% and 8% cases.

Micromachines now operate with longer lifetimes and greatly reduced wear

For more information:

Technical Contact:
Michael Dugger
505-844-1091
mtdugge@sandia.gov

Science Matters Contact:
Alan Burns
505-844-9642
aburns@sandia.gov

The development of complex micron-scale electromechanical devices, or MicroElectroMechanical Systems (MEMS), for weapons has been a very important and unique program at Sandia. An example of a tiny silicon-based mechanical device for weapon safety is shown in Figure 1. The ability to create this functionality with many moving parts at a size scale of millimeters means that safety and use-control systems can be implemented with much lower mass and volume. Commercial applications such as electromechanical locks for information access are also possible. However, due to the small scale, adhesive forces between contacting areas, such as electrostatic, van der Waals and capillary forces, become much more significant and tend to overwhelm the small actuation and mechanical restoring forces. Thus, in order to have reliable, freely-operating MEMS, the contacting surfaces must be "lubricated." Many schemes of lubrication via chemisorbed organic layers have been tried, but the durability of the layers has been insufficient to withstand repeated mechanical contact (Reference 1).

Now a new method to reliably lubricate silicon MEMS has been developed by Sandia and Pennsylvania State University. It can be replenished and does not rely on bulk liquids that introduce viscous losses. "Vapor phase lubrication," or VPL (Reference 2), takes advantage of the adsorption behavior of certain molecules on oxide surfaces, and the physical properties of their condensed phases. At concentrations between 10% and 90% of their saturation pressures, gaseous linear alcohols with three to ten carbon atoms adsorb on oxide surfaces with a thickness of two monolayers or less. This means that pentanol, for example, can maintain monolayer adsorption at a concentration of 400 parts per million (ppm) in an inert gas. When sliding of silicon takes place in this environment, extraordinarily low wear results (Figure 2). MEMS devices operated in this environment exhibit unprecedented operating life. The device in Figure 1 operating in 400 ppm pentanol vapor, was stopped for inspection after running for half a billion revolutions, with no detectable wear.

Sandia National Laboratories

LDRD LABORATORY DIRECTED RESEARCH & DEVELOPMENT

Several other types of silicon devices have been operated using alcohol for VPL, with similar results. Also, surface chemical analysis with high spatial resolution, surface sensitivity and chemical specificity is essential for understanding the reactions taking place during VPL. For example, Figure 3 demonstrates that the same chemical processes that occur in macroscale sliding tests (Figure 2) are also happening at the MEMS scale. Pin-on-disk measurements suggest that this lubrication approach also works on stainless steel surfaces.

Application of VPL to electromechanical devices critical to Sandia's mission is promising, and significant basic research and technology maturation are ongoing. The overall effort is to understand the surface chemistry, to tailor the vapor species for particular surfaces, to produce lower friction response, and to develop robust delivery schemes so that the environment for VPL can be produced and maintained over the desired operating temperature range.

References

1. D.A. Hook, S.J. Timpe, M.T. Dugger and J. Krim, "Tribological Degradation of Fluorocarbon Coated Silicon Microdevice Surfaces in Normal and Sliding Contact," *J. Applied Physics* **104** (2008) 034303.
2. D.B. Asay, M.T. Dugger, J.A. Ohlhausen and S.H. Kim, "Macro- to Nanoscale Wear Prevention via Molecular Adsorption," *Langmuir* **24** (2008) pp.155-159

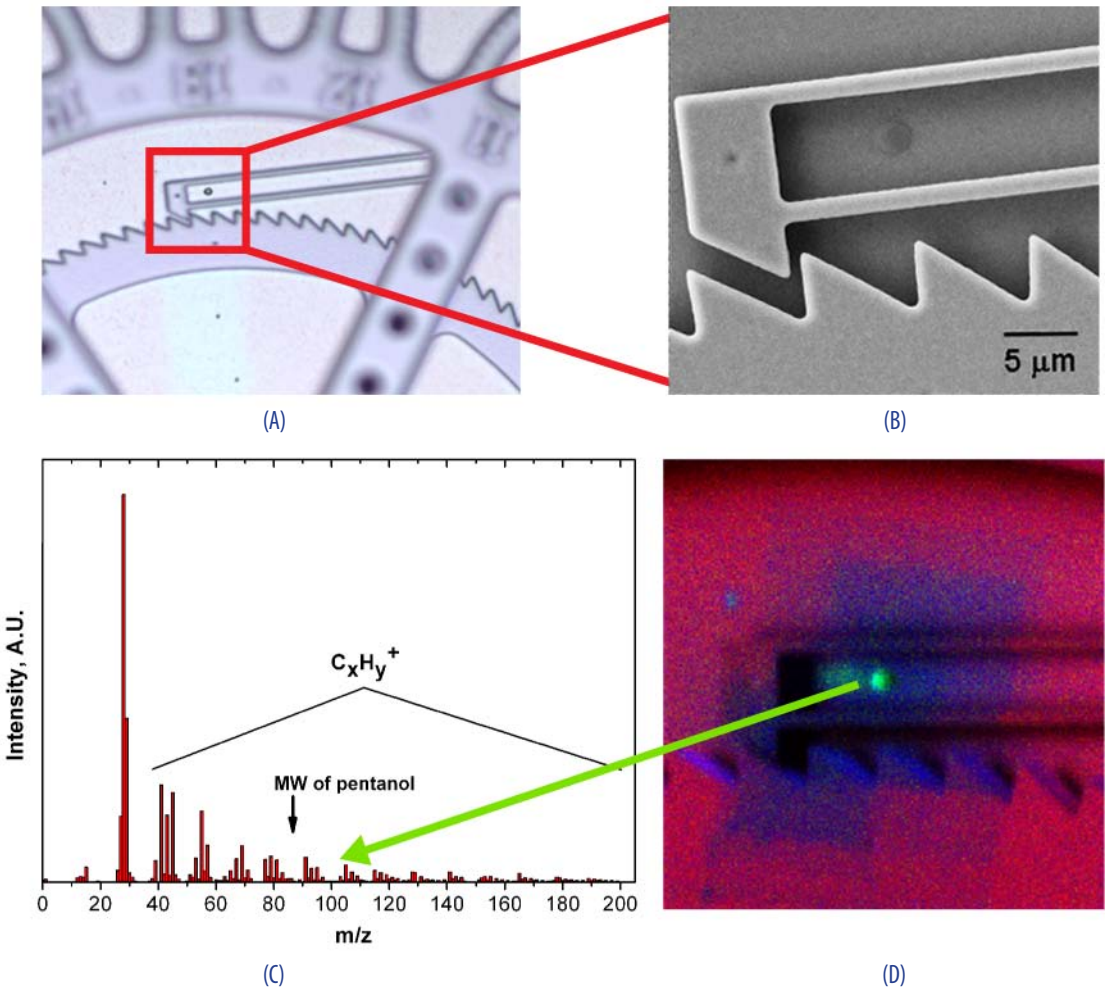

Figure 3: (A) Section of a MEMS rotary actuator operated $5x10^8$ revolutions in pentanol vapor, showing the thermally-actuated tooth (B) that engages the wheel for rotation. (C) The time-of-flight secondary ion mass spectroscopy corresponding to surface reaction products , and a spatial map of the reaction product (green area in D).

Microanalysis and the FBI's Investigation of the 2001 Anthrax Attacks

"Amerithrax" investigation asks Sandia to perform detailed forensic analyses to help determine methods of manufacture

For more information:

Technical Contact:
Paul G. Kotula
505-844-8947
pgkotul@sandia.gov

Joseph R. Michael
505-844-9115
jrmicha@sandia.gov

Science Matters Contact:
Alan Burns
505-844-9642
aburns@sandia.gov

The anthrax attacks of 2001 in the U.S. killed five, sickened twenty-two others, and caused a significant disruption of mail and other government facilities. Although some of the attack materials (*Bacillus anthracis*) were recovered in powder form in sealed envelopes, the US Federal Bureau of Investigation (FBI) was unprepared to perform the needed forensic analyses on these bio-weapon substances. In particular, they realized that analysis from the micro- to nano-scale was a key missing piece of their capabilities. As a result, Sandia was asked to analyze the materials from the attacks and report findings by early 2002; Sandia was able to submit an initial report within a few months. A more detailed investigation was carried out subsequently, and finally concluded in 2008. Over 200 samples of *B. anthracis* were analyzed in an attempt to discern the method of manufacture of the attack materials. After so many years, Sandia is now able to discuss this previously classified research.

Sandia's long expertise in the development and application of microanalysis techniques, available only at Sandia at the time, led the FBI to ask for its involvement in their investigation. They asked Sandia to answer several critical questions, including: Was the *B. anthracis* treated to make it more lethal? Were the materials in the various attacks from the same source? Three primary microanalysis techniques, combined with multivariate statistical analysis [References 1-3], were used to answer these questions: (1) x-ray spectral imaging, where a complete x-ray spectrum is acquired from each point in an array, (2) scanning electron microscopy (SEM), and (3) scanning transmission electron microscopy (STEM). Figure 1a is a STEM image of a fixed, stained, and microtomed section of *B. anthracis* spores from the letter sent to the *New York Post*. The spores had not been treated with silicon oxide (Si-O) nanoparticles that have been typically used as dispersal agents to make the substance more lethal. Figure 1b is an SEM image of a clump of spores from the letter sent to Senator Leahy where there is no extraneous material visible at these length scales. Further analyses of material from the letter sent to Senator Daschle show similar results. Detailed microanalysis, as shown in Figure 2, did indicate the presence

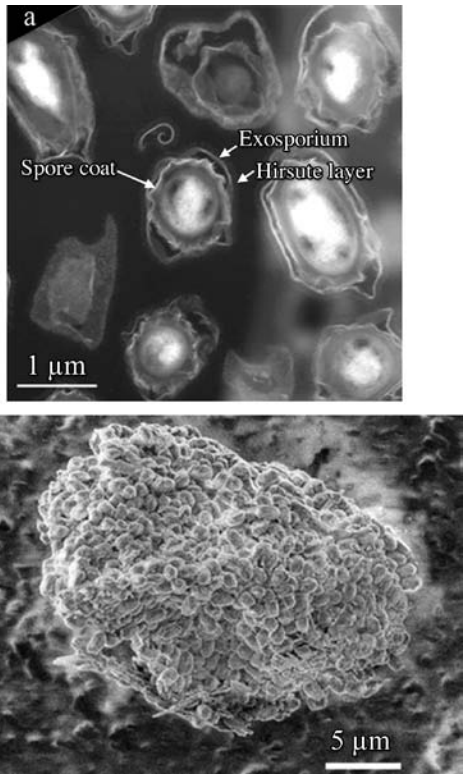

Figure 1: a) Annular dark-field STEM image of a fixed and stained, microtomed section of *B. Anthracis* from the *New York Post* letter. b) SEM image of a clump of *B. Anthracis* spores from the Leahy letter.

Sandia National Laboratories

National Nuclear Security Administration

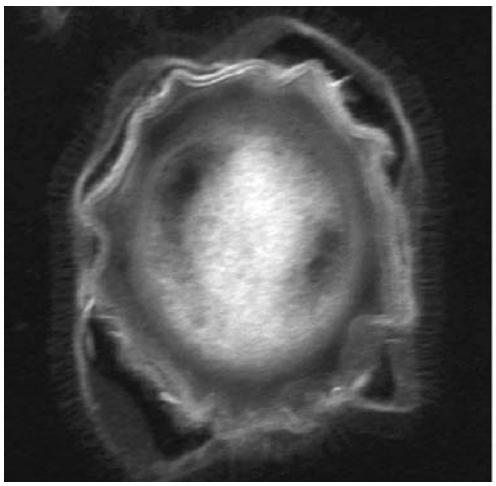

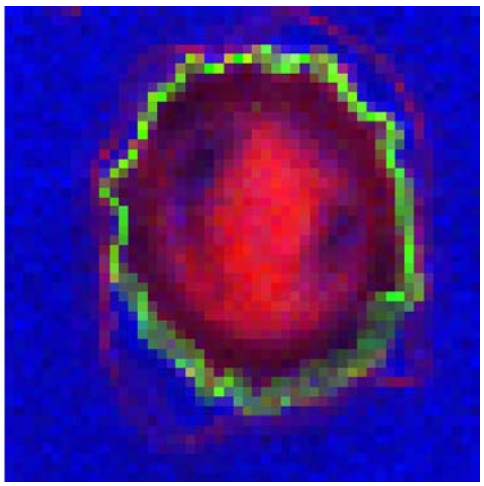

Figure 2: Annular dark-field STEM image of a single spore from the *New York Post* letter (left), and microanalysis results (right) showing that Si-O (green) is present on an internal spore structure, namely the spore coat. Red corresponds to the fixing/staining materials (osmium, uranium, and lead) while blue corresponds to the plastic in which the spores were embedded for microtoming. Image widths are 1.5 µm.

of Si-O in the attack materials. However, it was associated with an internal structure of the spores, and was thus related to the growth method, rather than added post-sporulation for enhanced dispersion. The chemical signature of the spore coat of the attack materials included not only silicon and oxygen as major elements, but also minor amounts of iron and tin. All of the attack materials examined by Sandia shared this common signature, thus indicating that they were most likely produced by the same method and probably from the same source.

References

1. P.G. Kotula, M.R. Keenan and J. R. Michael, "Automated Analysis of SEM X-Ray Spectral Images: A Powerful New Microanalysis Tool," *Microsc. Microanal.* **9**, 1-17 (2003).
2. P.G. Kotula and M.R. Keenan, "Application of Multivariate Statistical Analysis to STEM X-Ray Spectral Images: Interfacial Analysis in Microelectronics," *Microsc. Microanal.* **12**, 538-544 (2006).
3. L.N. Brewer, J. A. Ohlhausen, P.G. Kotula, and J.R. Michael, "Forensic analysis of bioagents by X-ray and TOF-SIMS hyperspectral imaging," *Forensic Science International* **179** 98-106 (2008).

Stretching Table Salt into Superplastic Nanowires

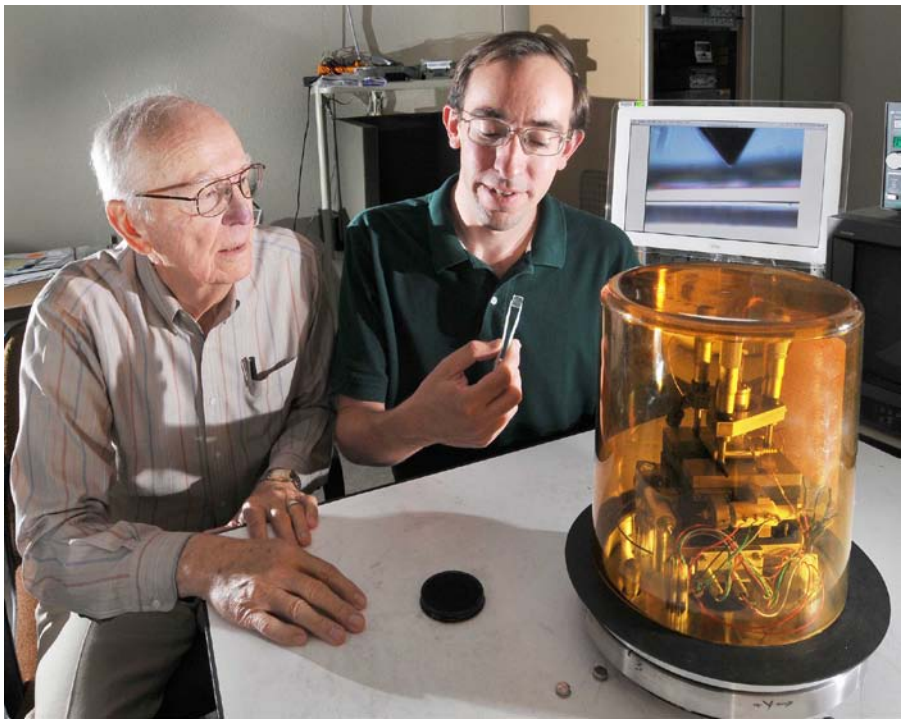

Figure 1: Two of the Sandia researchers, Jack Houston (left) and Nathan Moore (right) examine a salt crystal studied in the IFM instrument (foreground) using the diamond probe tip (magnified on screen, back).

Normally brittle material stretches like taffy in the nanoworld

For more information:

Technical Contact:
N. Moore
505-844-0278
nwmoore@sandia.gov

J. Huang
505-284-5963
jhuang@sandia.gov

Science Matters Contact:
Alan Burns
505-844-9642
aburns@sandia.gov

Although everyone is familiar with common salt (sodium chloride), relatively little is known about how it impacts daily lives at the length scales of atoms and molecules. Ions and nanometer-sized crystals of sodium chloride play key roles in applications like water purification, the stability of rock salt for carbon sequestration and underground nuclear waste disposal, and for seeding atmospheric reactions. For example, it is now recognized that changes in crystal morphology can affect the reactions of sea salt aerosols, which have been implicated in problems as broad as smog formation, ozone destruction, and triggering asthmatic responses in humans.

Experiments originally aimed at understanding how water bonds to salt surfaces for desalination applications led to the surprising discovery that superplastic nanowires were being pulled from the surface of ordinary table salt. In the initial experiments, the Sandia-developed interfacial force microscope (IFM, Figure 1) showed an unusual adhesive force when a sharp diamond tip approached within a few nanometers of a salt crystal. This adhesive force remained as the tip withdrew, suggesting that the tip was pulling long tendrils of salt from the crystal surface. Similar adhesion experiments with sharp gold tips in a transmission electron microscope (TEM) confirmed that superplastic nanowires were being pulled from the salt surface (Figures 2, 3). The nanowires stretched ~2.2 μm, or 280% of their original length, and could be bent >90° upon compression. The nanowires necked down, rather than fracturing, as if the salt crystal were more akin to chewing gum than a rigid solid.

Superplasticity, or elongation to failure >100%, is a rare material property at room temperature, and even more rare for ionic crystals, having been seen for only a few

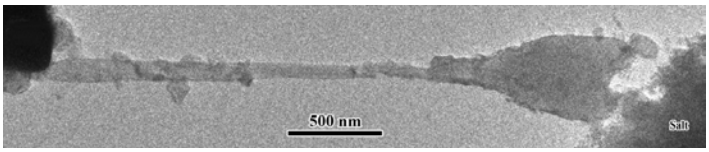

Figure 2: TEM image of a typical salt nanowire created after touching a gold tip to a salt crystal.

compounds. That table salt can stretch into nanowires comes as a surprise, because one is accustomed to the tiny salt crystals shaken onto food, and which appear brittle and shatter like glass into small pieces upon crushing.

One key to understanding the super-elongation is the disruption of the regular arrangement of Na^+ and Cl^- ions in the salt crystal lattice. In the TEM measurements, the electron beam used to image the sample creates holes in the crystal lattice, opening spaces for ions to rapidly migrate and "heal" the nanowire as it elongates. Chemical analysis shows that the beam also reduces a small fraction of the Na^+ ions in the salt to metallic sodium (Na), which enhances the ductility of the wire. In the IFM experiments, mechanical and adhesive perturbations are believed to alter the crystal lattice near the surface where the nanowires form.

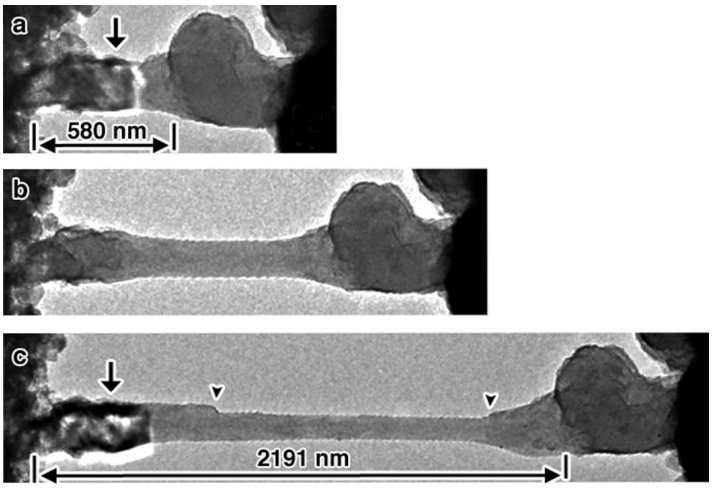

Figure 3: Time-lapsed TEM images showing super-elongation of a nanowire (a → c; time = 0, 256, and 502 sec., respectively). The gold tip (not shown) is adhered to the NaCl grain at the right side of these images. Arrows point to examples of steps and crystalline contrast on the nanowire surface. Roughness of the NaCl surface (left) appears exaggerated by the transverse imaging direction, which contracts the image.

This is the first demonstration of superplasticity in an ionic material at the nanoscale. Other materials that neck into nanowires far below their melting point have all been metals (e.g., gold, lead). Furthermore, the behavior of low-temperature-deforming, one-dimensional nanomaterials, such as carbon nanotubes and ceramic nanowires, would not have predicted similar behavior in ionic nanowires. The discovery may inspire new ways to create nanostructures through mechanical pulling or dissolvable templates. This work also raises broad questions about the presence of nanomaterials in the environment and their unseen influences. More fundamentally, the idea that common salt can be superplastic is a striking and unexpected example of how material properties can change when structures are reduced to nanoscale dimensions.

Reference

N. W. Moore, J. Luo, J. Y. Huang, S. X. Mao, and J. E. Houston, "Superplastic Nanowires Pulled from the Surface of Common Salt," *Nano Letters* **9(6)**, 2295 (2009).

Metamaterial Science and Technology

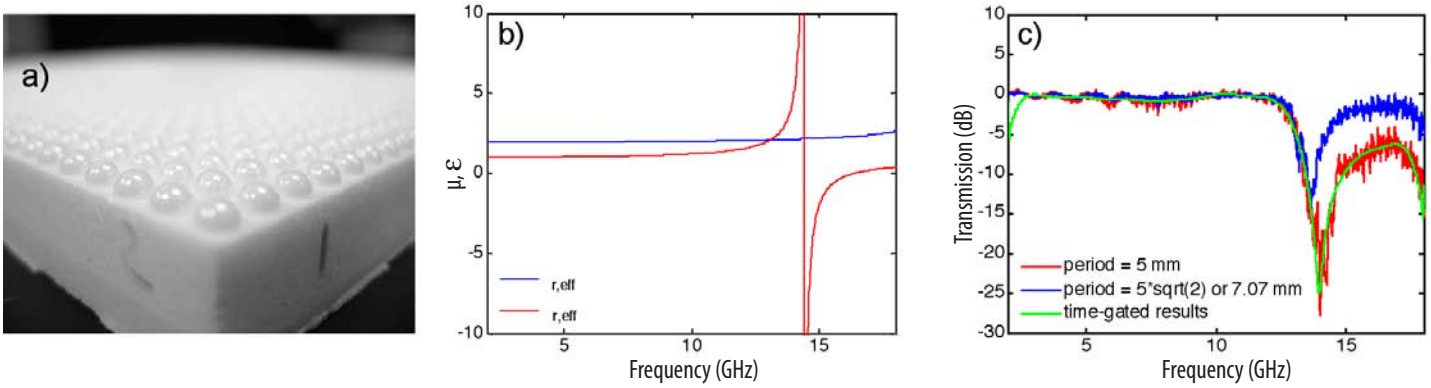

Figure 1: a) A photograph of a dielectric sphere-based RF metamaterial. b) Results of a numerical simulation of the effective electric permittivity and magnetic permeability of the array. Note the region of negative permeability just below 15 GHz. c) The measured RF transmission through the array. The observed stop band is in close correspondence with the predicted region of negative permeability.

Sandia researchers are designing new structures that have unusual optical properties

For more information:

Technical Contact:
Mike Sinclair
505-844-5506
mbsincl@sandia.gov

Science Matters Contact:
Alan Burns
505-844-9642
aburns@sandia.gov

Metamaterials form a new class of artificially-structured materials that provides the device designer with the ability to manipulate the flow of electromagnetic energy in ways that are not achievable with naturally-occurring substances. Recent theoretical investigations have predicted several astonishing applications, ranging from electromagnetic cloaking (rendering objects "invisible") to sub-diffraction limited imaging, that would become possible if the underlying metamaterials could be developed to a sufficient level. However, in spite of these and other advances in metamaterial theory, progress toward practical implementation, particularly at infrared and visible frequencies, has been hampered by high absorption losses. A large majority of the metamaterial designs demonstrated to date rely on the use of metallic structures and operate in the radio frequency (RF) range, where losses are significant but not insurmountable. However, as the frequency of operation is pushed towards the infrared and visible, ohmic losses quickly render current metamaterial approaches impractical.

Sandia has embarked on an ambitious research program to develop useful 3D metamaterials operating in the thermal infrared (8–12 μm). If successful, scientists will have the capability to arbitrarily engineer key optical material properties which will enable new optical designs and devices that can dramatically lower the size, weight, and power needed for national security and other applications. A top priority of this program is to reduce the absorption losses to levels suitable for device applications. This will require metamaterial designs that do not depend solely on metallic structures. One proposed approach is to utilize sub-wavelength arrays of dielectric resonator structures such as spheres (Reference 1). Through appropriate selection of the material and dimensions, resonators can be designed to exhibit either electric or magnetic dipole resonances at the desired operating frequency, thereby producing an effective electric permittivity or magnetic permeability that can be continuously tuned from positive to negative values. This approach can be readily verified through the design, fabrication, and characterization

Sandia National Laboratories

LDRD LABORATORY DIRECTED RESEARCH & DEVELOPMENT

of metamaterials operating at RF frequencies, and then extended to the thermal infrared. As an initial test, several metamaterials operating in the RF have been developed. Figure 1a shows an array of 4 mm diameter zirconium dioxide (ZrO_2) spheres (ε_r=25) contained in a computer-numerical-controlled machined RHOACELL® foam template. This array is designed to exhibit a magnetic dipole resonance near 14 GHz (Figure 1b). The measured RF transmission through the array (fig 1c) shows a deep transmission null near 14 GHz that corresponds to the spectral range where the effective magnetic permeability is negative.

In principle, simultaneous tuning of both the permittivity and permeability can be achieved through the use of a unit cell design that incorporates both electric and magnetic dipole resonators. To test this concept, Sandia researchers have designed (Reference 2) an isotropic, low-loss, negative index metamaterial, in which both the permeability and permittivity exhibit negative values at the RF operating frequency (Figure 2). The spheres colored in blue have a radius of 2 mm, and are designed to exhibit an electric dipole resonance near 17 GHz. The spheres colored in pink have the same radius, but are fabricated from a different material so that they exhibit a magnetic dipole resonance at the same frequency. Because the spheres are arrayed with a sodium chloride (NaCl) cubic crystal structure, the response of the metamaterial is expected to be isotropic with respect to the direction of propagation of the electromagnetic wave. This metamaterial has been fabricated using spheres made from selected microwave ceramics and its RF transmission characteristics are currently being measured. Research is now focusing on preparing infrared metamaterials that employ the same concepts.

References

1. C.L. Holloway, E.F. Kuester, J. Backer-Jarvis, and P. Kabos, "A double negative (DNG) composite medium composed of magnetodielectric spherical particles embedded in a matrix", IEEE Trans. on Antennas and Propagation, vol. 51, pp. 2596-2603, 2003.
2. J. H. Loui, J. Carroll, P. Clem and M. Sinclair, "Experimental realization of low-loss 3D isotropic DNG materials", proceedings of MM09, Sept. 2009, London, UK.

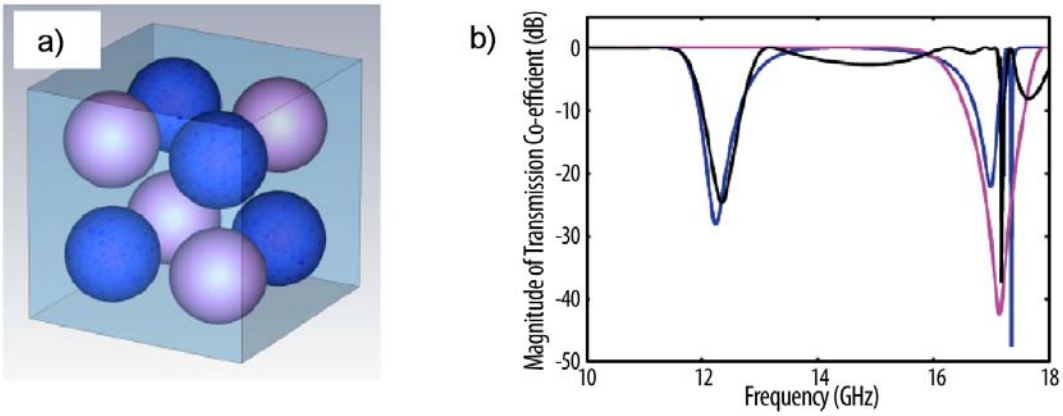

Figure 2: a) A metamaterial unit cell containing both electric (blue) and magnetic (pink) dipole resonators. The spheres are arrayed with the NaCl crystal structure to promote isotropic response. b) Results of a numerical simulation of the transmission through metamaterials containing only electric resonators (blue line), magnetic resonators (pink line), and the composite metamaterial containing both blue and pink spheres (black line). The region of high transmission near 17 GHz occurs where both the effective permittivity and permeability are negative and corresponds to a region of negative index behavior.

Red-Emitting Phosphors for White Light-Emitting Diodes

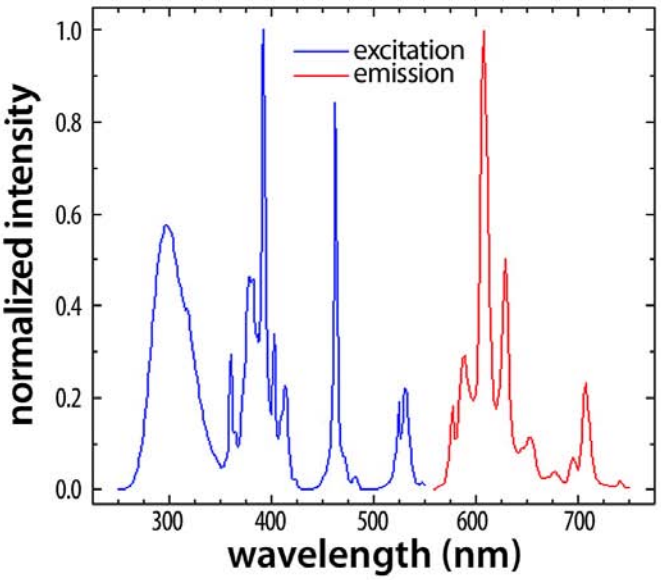

Figure 1: Photoluminescence excitation and emission spectra of Eu^{3+}-doped lutetium tantalate phosphor.

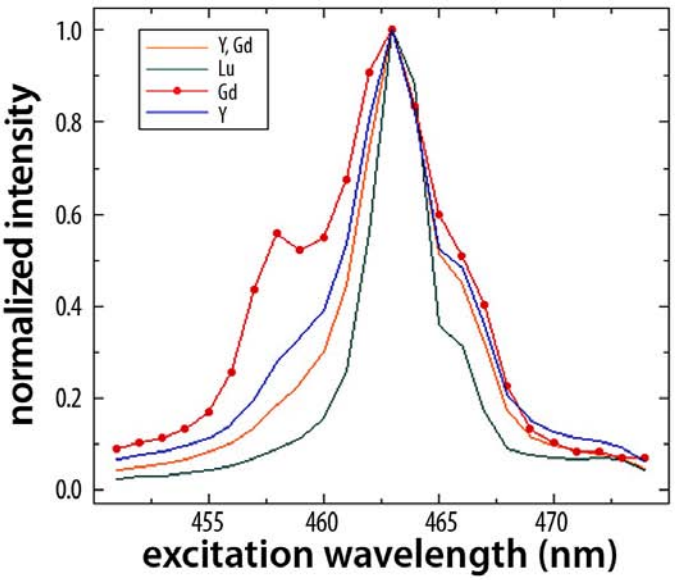

Figure 2: A comparison of the blue excitation peaks of the various rare-earth tantalates shows that the Gd phosphor has a significantly larger excitation bandwidth.

"Warm" white light achievable with new rare-earth structures

For more information:

Technical Contact:
Lauren Rohwer
505-844-6627
leshea@sandia.gov

Science Matters Contact:
Alan Burns
505-844-9642
aburns@sandia.gov

Sandia has developed red-emitting phosphors that will help to transform the cold blue of many current light-emitting diodes (LEDs) into the warm white that is preferred for general lighting. This advance could help move solid-state lighting (SSL) into broader applications and market spaces.

The solid-state devices that have been targeted use the nearly monochromatic blue emission from InGaN (indium gallium nitride) LEDs to excite yellow-green emission from Ce^{3+}-doped yttrium aluminum garnet (YAG:Ce) phosphors. These devices produce light in the blue to yellow portion of the visible spectrum, which means that orange or red objects appear dim and colorless under this lighting. Thus to improve their white light quality, these devices require red-emitting phosphors that can be excited by blue LEDs. Thanks to researchers at Sandia, such a family of phosphors is now available.

Most red phosphors are doped with Eu^{2+} ions whose emission is due to parity-allowed 5*d*-4*f* transitions. The 5*d* orbitals are spatially diffuse and their energy levels strongly depend on the local crystal field of the surrounding ions in the lattice. This leads to emission band broadening because of both differences in the atomic environments (inhomogeneous broadening) and phonon coupling (homogeneous broadening). An undesirable consequence of broad emission is deep-red emission, to which the eye is insensitive. The absorption bands are also broad, enabling excitation with near-UV to visible LEDs, but also unwanted absorption of green or yellow emission from other phosphors in the blends. For these reasons, Sandia has focused on narrowband red-emitting phosphors with narrowband blue absorption for SSL applications.

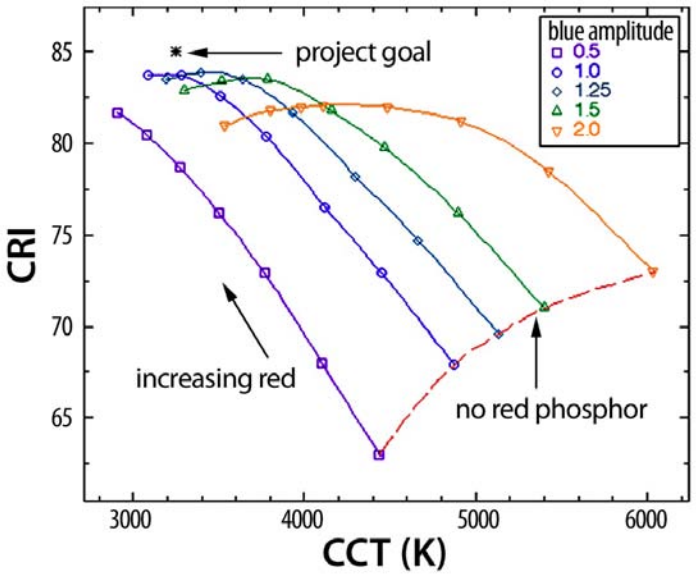

Figure 3: Color quality calculations for luminaires consisting of a 465 nm LED pumping YAG:Ce and Eu^{3+}-doped tantalate blends. The blue amplitude is relative to the amplitude of the YAG:Ce emission (peak to peak). The red dashed line is the locus of points without the red phosphor; decreasing the blue emission reduces the CCT, but at the price of drastically reducing the CRI. At any given blue/YAG:Ce ratio, adding the red emission decreases the CCT while increasing the CRI.

It was discovered here that Eu^{3+} in rare-earth (RE) tantalate phosphors with the pyrochlore structure, $K(RE)Ta_2O_7$ (RE=Gd, Lu, or Y), can be excited directly with blue LEDs to produce narrowband red emission with efficiencies of nearly 80%, more than three times that obtained from conventional Eu^{3+}-doped phosphors (Reference 1). This narrowband emission is due to parity-forbidden 4*f*-4*f* transitions that are weakly dependent on the crystal field, but are sensitive to the symmetry of the Eu^{3+} site. The pyrochlore structure is highly flexible, offering much greater control over site symmetry than the zircon-type structures of conventional phosphor lattices. The ability to control the site symmetry enables a scientific approach to the development of a useful red phosphor. Thus by altering the oxygen vacancy concentration and the geometry of the Eu^{3+} site, Sandia can tailor the structure in order to decrease the centrosymmetry at each Eu^{3+} location.

These new materials have intense emission at ~610 nm - an ideal wavelength for warm white LEDs (Figure 1). The blue excitation linewidth is important for SSL applications. Figure 2 shows the blue excitation peak for different rare-earth tantalates. The linewidth of the Gd phosphor is nearly twice that of the Lu phosphor. This increased linewidth reduces the need for stringent emission wavelength control of the LEDs, and increases the absorption cross section of the phosphor. Calculations of the color rendering index (CRI) and correlated color "temperature" (CCT) for theoretical blends of blue LED, YAG:Ce, and red tantalate emissions are summarized in Figure 3. Without the red phosphor, the CRI is 73 at a CCT of 6000 K, and the CRI falls to 68 if the YAG emission is increased to give a CCT of 5000 K. Further decreases in the CCT lead to even lower CRIs. By adding the red phosphor, computer simulations indicate that a CRI of 85 at a CCT of 3250 K is achievable, satisfying the criteria of warm white light. The goal is to meet or exceed this color quality in an operating device.

Reference

1. M. Nyman, M.A. Rodriguez, L.E. Shea-Rohwer, J.E. Martin, P. Provencio, "Highly versatile rare-earth tantalate pyrochlore nanophosphors," *J. Am. Chem. Soc.*, ASAP Web release, July 31, 2009.

Nanowire Templated Lateral Epitaxial Growth of High Quality GaN

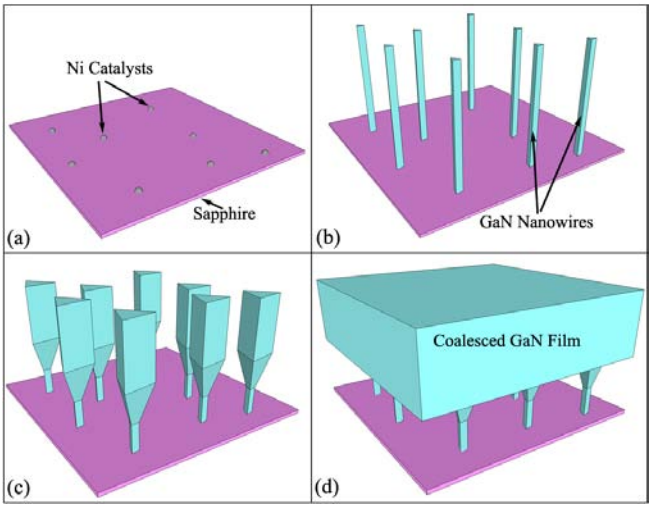

Figure 1: NTLEG growth process. (a) catalyst nucleation; (b) vertically-aligned nanowire growth; (c) lateral growth; and (d) full coalescence of the upper section into a suspended GaN film that is bridged to the substrate by the nanowires.

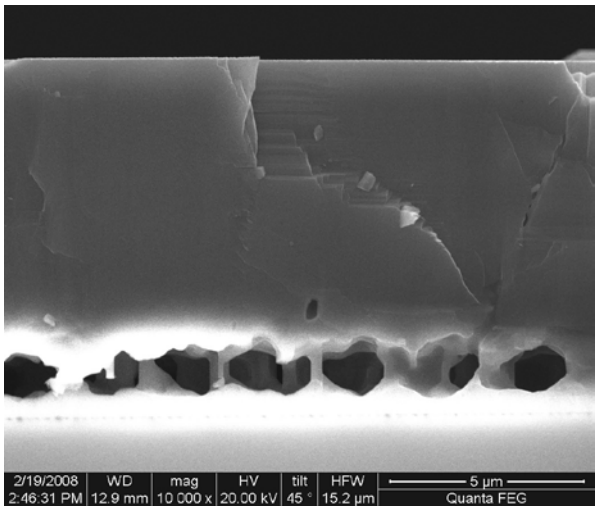

Figure 2: Cross-section scanning electron micrograph showing a fully-coalesced GaN film bridged to the sapphire substrate via vertically-aligned GaN nanowires.

New technique may improve performance of energy-saving solid-state lighting devices

For more information:

Technical Contact:
George T. Wang
505-284-9212
gtwang@sandia.gov

Science Matters Contact:
Alan Burns
505-844-9642
aburns@sandia.gov

Artificial lighting consumes about 20 percent of electricity in the U.S., due in large part to the poor energy efficiency of incandescent bulbs. A potential solution resulting in huge future energy savings is found in the much more efficient solid-state lighting (SSL). At the heart of SSL is the light-emitting diode (LED), a device which typically consists of a sandwich of gallium nitride (GaN)-based semiconductor layers that emits visible light when electrically driven. Most LEDs are grown on crystalline substrates such as sapphire, because bulk GaN crystals are difficult to grow. Unfortunately, the large lattice mismatch, or difference in atomic spacing, between GaN and the sapphire results in the formation of very high densities (~1 billion/cm^2) of extended defects (threading dislocations) in the GaN layers. These defects significantly degrade the efficiencies and lifetimes of visible LEDs, and thus hinder the development of high performance SSL.

At Sandia, researchers have developed an innovative and inexpensive technique to produce high-quality, relatively defect-free GaN on sapphire substrates by employing aligned arrays of single-crystalline GaN nanowires as templates (Reference 1). In this technique, called nanowire-templated lateral epitaxial growth (NTLEG) and illustrated in Figure 1, a vertical and dense array of aligned GaN nanowires is first grown on sapphire by a metal-catalyzed metal-organic chemical vapor deposition process. The growth conditions are then changed *in-situ* to quench axial nanowire growth and nucleate lateral GaN film growth at the upper part of the nanowire template until a coalesced film is formed. This continuous suspended GaN film is bridged to the substrate by the GaN nanowire array, as shown in a cross-section electron micrograph (Figure 2).

Sandia National Laboratories

LDRD LABORATORY DIRECTED RESEARCH & DEVELOPMENT

The GaN nanowires (Figure 3) have a number of unique properties that lead to the reduction in defects in the GaN films grown by this technique. Because of their small dimensions (typically less than 100 nm diameter) and 1D-like morphology, the nanowires can relax laterally to relieve the strain caused by growth on lattice mismatched substrates. Since strain is the primary cause of defects, this results in GaN nanowires that are free of threading dislocations, providing a high-quality template for GaN film growth. Additionally, this property allows the nanowires to serve as a strain-compliant bridge from the coalesced GaN film to the lattice-mismatched substrate. Finite element models (Figure 4) show that the strain caused by the lattice mismatch of GaN and sapphire decays exponentially from the nanowire-sapphire interface, and is dissipated away from the suspended GaN film. Structural analysis of preliminary GaN films (Figure 5) shows an approximate fifty times reduction in threading dislocation density compared to films of the same crystal orientation grown by conventional buffer-layer techniques; further optimization of the technique is expected to result in additional gains. In addition to better LEDs for more efficient SSL, this technology could also lead to improvements in other GaN-based technologies including blue laser diodes (e.g., Blu-Ray) and high-speed, high-power electronics.

Reference

1. Q. Li, Y. Lin, J. R. Creighton, J. J. Figiel, G. T. Wang, "Nanowire-templated lateral epitaxial growth of low-dislocation density nonpolar a-plane GaN on r-plane sapphire", *Adv. Mater.* **2009**, *21*, 2416.

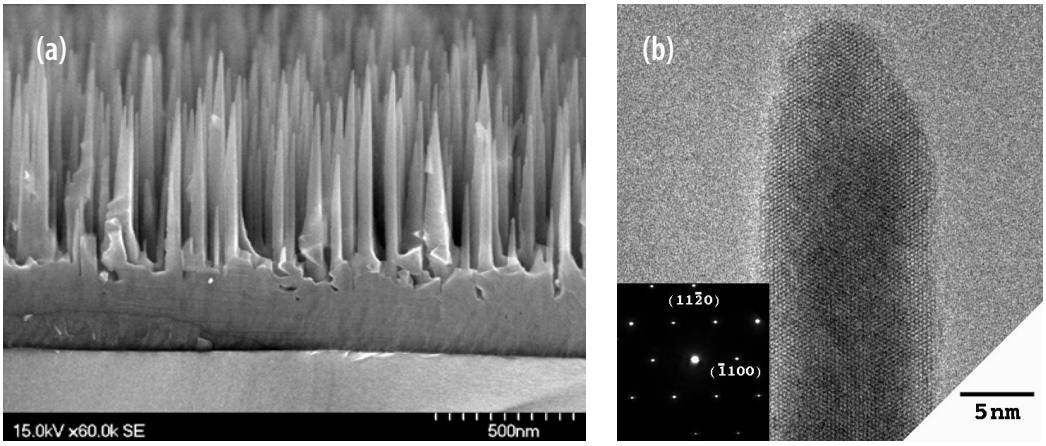

Figure 3: (a) Scanning electron micrograph showing highly-aligned and dense GaN nanowire growth on sapphire; (b) transmission electron micrograph and diffraction pattern (insert) showing single-crystalline, dislocation-free structure of a GaN nanowire.

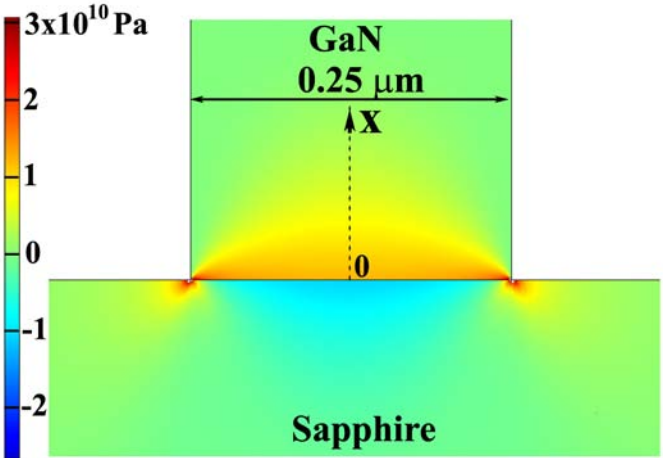

Figure 4: Finite element analysis of lattice mismatch strain distribution in a 0.25-μm-wide GaN nanowire on bulk sapphire substrate, showing rapid strain relaxation in the nanowire away from the interface.

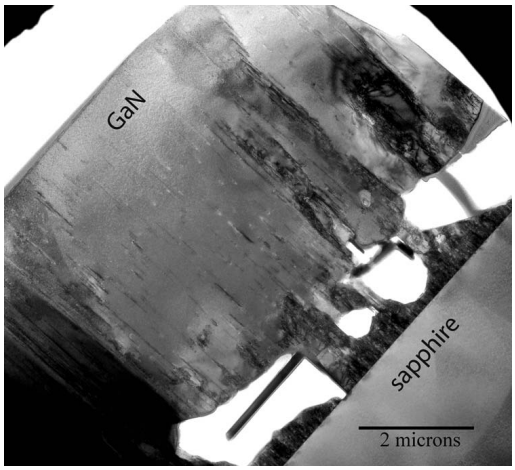

Figure 5: Cross-section transmission electron micrograph showing a large reduction in threading dislocations (denoted by dark striations) near the top of the suspended GaN film compared to the highly-defective, high-strain region near the nanowire/sapphire interface.

Engineered Neural Networks using Microfabricated Cell Guidance Cues

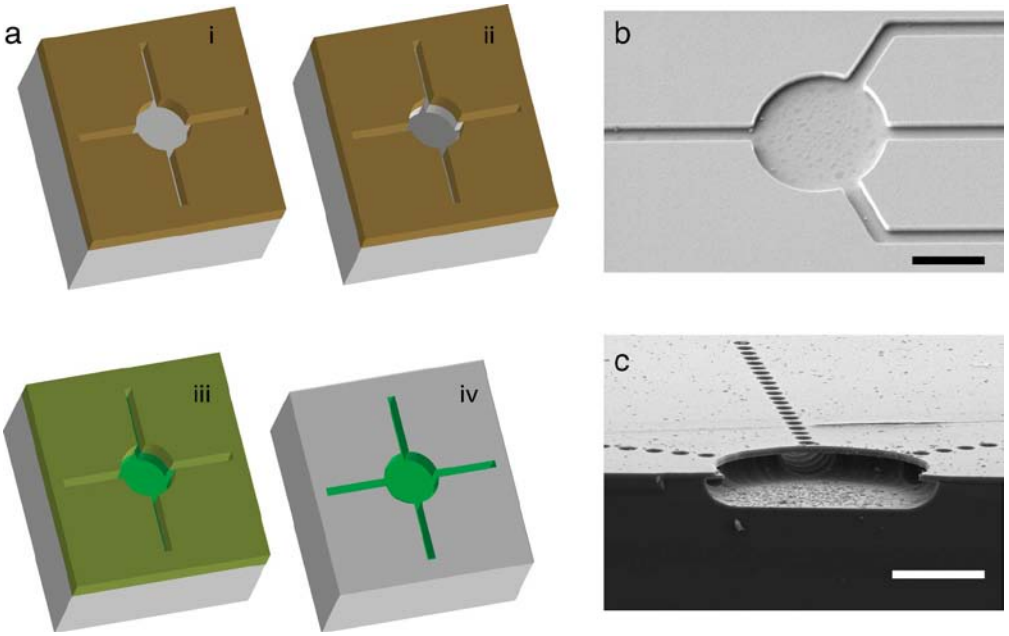

Figure 1: (a) Dual chemical and topographical guidance cue substrate preparation: (i) resist patterning, (ii) reactive ion etching of the glass substrate, (iii) adsorption of adhesive molecules, and (iv) acetone liftoff to remove the resist. (b) Reactive ion etched cell guidance cues. (c) Wet hydrogen fluoride etched buried guidance cues. Scale bars=10 µm.

Precise organization of neurons will ultimately help the understanding of brain function

For more information:

Technical Contact:
Conrad James
505-284-9546
cdjame@sandia.gov

Science Matters Contact:
Alan Burns
505-844-9642
aburns@sandia.gov

In order to test hypotheses regarding the relationship between brain network architecture and function, researchers require the ability to engineer, measure, and modify living neural networks in controlled environmental conditions. Eventually, such technology could provide the capability to repair damaged nerve tissue and fully restore lost motor, sensory, and cognitive functions. However, current neural engineering efforts organize large populations of neurons into grossly-defined patterns with minimal success at organizing individual synaptic connections (Reference 1). These connections are the key element of circuit connectivity and functionality, thus the objective here is to develop microfabrication methods for precisely organizing neurons into functional networks.

Specifically, Sandia is interested in monitoring the development of long-term potentiation (LTP) and long-term depression (LTD) in engineered networks of rat neurons. LTP and LTD are phenomena whereby stimulated neurons maintain a change in their electrical output after the cessation of stimulation, and these mechanisms are believed to underlie memory and learning *in vivo*. The synaptic interface between neurons will be controlled and varied with microfabricated cell guidance cues (Reference 2) in order to determine the influence of network architecture on the development of LTP and LTD. These cues contain patterned chemical and topographical features that promote neuron attachment (e.g., chemically via the charged amino acid poly-lysine) and outgrowth at pre-defined locations. Fabrication of these devices is shown in Figure 1. A working example is shown in Figure 2, where simple changes in guidance cue geometry controls the polarity of neurons. Figure 2c shows that optimized geometry of the guidance cues can be used

Sandia National Laboratories

LDRD LABORATORY DIRECTED RESEARCH & DEVELOPMENT

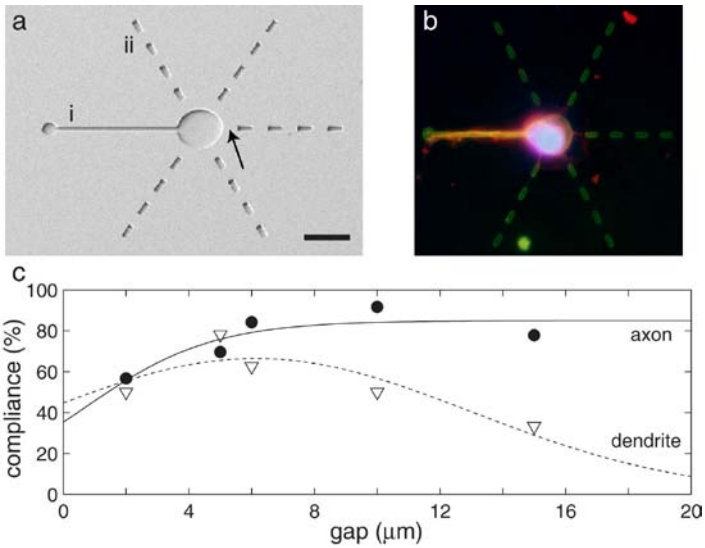

Figure 2: (a) Guidance cues for controlled neuron polarization. Continuous features (i) for directing axons and interrupted features (ii) for guiding dendrites are shown. (b) Fluorescence image of a properly polarized rat neuron. (c) Compliance of axons and dendrites as a function of the gap (arrow in a) between the node and the first interrupted feature.

to promote rapid neuron growth in one direction, which leads to axon development (electrical output), and to delay growth in other directions, which leads to dendrite development (electrical input).

Patch clamp and field recording electrophysiology are being used to measure the electrical response of engineered networks of neurons (Figure 3a). This system is capable of measuring microvolt changes in cell membrane potential, and, in conjunction with fluorescence probes, can be used to monitor coordinated activity such as calcium ion flow and action potential signaling. The experimental data is then used to train a computational model implemented in Sandia's custom circuit simulator program Xyce in order to predict network architectures that exhibit designed input/output characteristics. The ultimate objective is to decipher the mechanisms involved in human decision making, and to specifically understand the importance of the brain's corticostriatal networks in such cognitive processes. These networks integrate multiple sets of information (motor, sensory, cognitive, and reward); thus Sandia is constructing engineered corticostriatal networks and comparing the development of LTD/LTP in engineered networks to that measured in intact brain slices (Figure 3b).

Although just beginning, this work has resulted in additional projects. One is in collaboration with the University of Texas to study the repair of neuro-muscular junctions using neural engineering technologies. In another, funds from the Defense Advanced Research Projects Agency are being used to develop these microsystem techniques to engineer the hippocampal network, a region of the brain heavily involved in memory and learning.

References:

1. James, C.D, et al., IEEE Trans. Biomed. Eng. 2004; **51**, pp. 1640-1648.
2. Withers, G.S., James, C.D., et al., J. Neurobiology 2006; **66**, pp. 1183-1194.

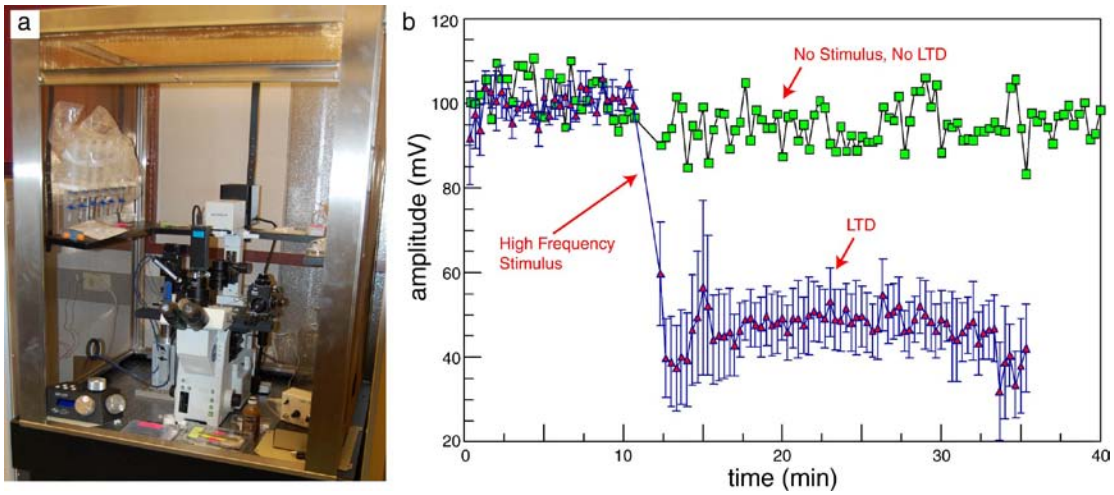

Figure 3: (a) Electrophysiology apparatus for monitoring electrical activity in living neural networks. (b) High-frequency stimulation-induced long-term depression measured in corticostriatal networks in a rat brain slice.

Measuring and Predicting Wind Turbine Aero-Acoustic Noise

Figure 1: View down the length of a Sandia BSDS rotor blade. The flatback airfoil shape is visible over the inboard portion of the blade.

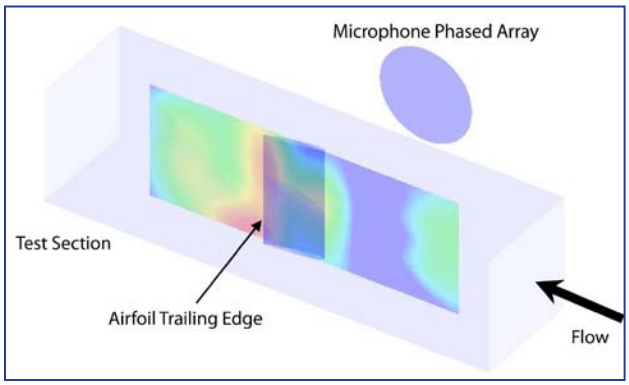

Figure 2: Wind tunnel configuration for measurement of aero-acoustic noise of a flatback airfoil. The microphone phased array measures the noise intensity emanating from locations within the test section. This intensity is visualized by the color contours on a plane passing through the airfoil model.

Advanced experimental and computational techniques are being used to reduce wind turbine noise

For more information:

Technical Contact:
Matt Barone
505-284-8686
mbarone@sandia.gov

Science Matters Contact:
Alan Burns
505-844-9642
aburns@sandia.gov

Wind turbines provide a rapidly growing portion of total electrical power generation in the United States, where, in 2008, 42% of newly installed generation capacity came from wind energy. Wind turbine manufacturers are careful to minimize the environmental impacts of their turbine designs, including those associated with acoustic noise. A primary source of noise on modern wind turbines is the "aero-acoustic" noise created by the motion of the rotating turbine blades relative to the surrounding air. The precise relation between the shape of a blade design and its aero-acoustic noise signature is not well understood, with the result that most blade designers are averse to making large design changes that may unintentionally increase the amount of noise.

Researchers at Sandia are using novel experimental and computational techniques to better understand and predict wind turbine aero-acoustic noise, with the twin goals of decreasing the cost of energy and the environmental impacts of future turbine designs. One focus is the characterization of the novel concept called the "flatback blade." The flatback concept is an innovative aero-structural blade design incorporating airfoil shapes with a blunt trailing edge into the inner portion of the rotor blades. The blunt shapes lead to a lighter, more efficient structure and improved aerodynamic properties. Sandia has designed and built a research rotor, called the Blade System Design Study (BSDS) rotor (Figure 1), that incorporates flatback airfoils along with other innovative structural concepts. Experiments were performed on a flatback airfoil in a special aero-acoustic wind tunnel at Virginia Tech that is outfitted with a sophisticated beam-forming microphone array for measuring flow-generated noise on airfoil models (Figure 2). The impact of a simple splitter plate attachment to the airfoil trailing edge (Figure 3) on the noise

Figure 3: Wind tunnel model of a flatback airfoil with a splitter plate attached to the trailing edge for noise reduction.

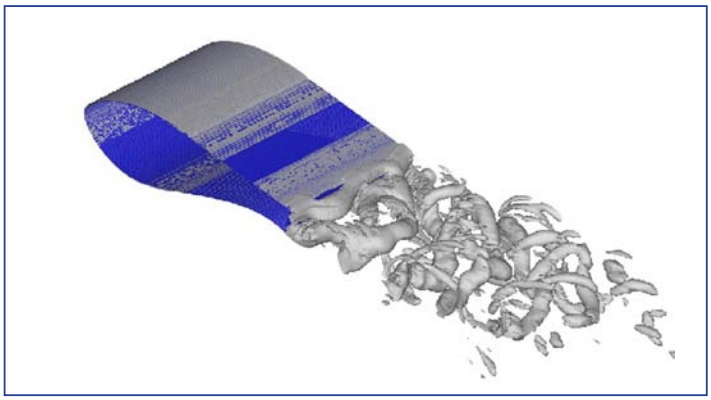

Figure 4: CFD prediction of the flow near the trailing edge of a flatback airfoil. The grey iso-contours highlight regions of rotational flow that interact with the trailing edge to produce aero-acoustic noise.

was also investigated, and found to decrease the peak noise amplitude by 12 dB (a difference approximately equivalent to the difference between the noise from busy street traffic and noise from a normal conversation). Data from the wind tunnel experiments are being used to validate Computational Fluid Dynamics (CFD) models of both the airfoil aerodynamics and of the aero-acoustic noise (Figure 4).

Aero-acoustic measurements are also being made of the noise generated by the BSDS rotor on a 100 kW Sandia test turbine (Figure 5) operated at the US Dept. of Agriculture wind turbine test site in Bushland, TX. Sandia is collaborating with staff from the National Renewable Energy Laboratory to apply a large-scale microphone array for field measurements of wind turbine noise. Much like the smaller array used in the wind tunnel experiments, this array is able to pinpoint the location of aero-acoustic noise sources on the rotor, while at the same time quantifying their amplitude and frequency. Measurements from this test will be used to quantify the noise associated with a flatback rotor in operation, as well as provide a valuable experimental database for validation of predictive models of wind turbine noise.

The knowledge of wind turbine blade noise gained from this research is eliminating barriers for new and innovative wind turbine blade concepts, such as flatback blades. These innovations promise future gains in turbine efficiency, reductions in turbine costs, and mitigation of environmental impact, all of which will help the wind industry make further progress in providing a renewable energy future for the U.S.

Reference

M. Barone and D. Berg. "Aerodynamic and Aeroacoustic Properties of a Flatback Airfoil: An Update." AIAA Paper 2009-271, presented at the 28th ASME Wind Energy Symposium, Orlando, FL, January 2009.

Figure 5: The BSDS rotor deployed in the field at the USDA test site in Bushland, TX. The microphone array for measuring wind turbine noise is located in the foreground, with 19 microphones located on the central platform and 19 additional peripheral microphones with locations marked by protective plastic covers.

A Framework for Critical Infrastructure Resilience Analysis

Sandia is working with the Department of Homeland Security to optimize infrastructure recovery strategies in the wake of natural disasters

The federal government's traditional policy toward critical infrastructure security is one of physical protection and "hardening" of infrastructure assets (e.g., electricity, water supply). In recent years, the Department of Homeland Security (DHS) has recognized that "protection, in isolation, is a brittle strategy," and that critical infrastructure protection policies should consider not only the prevention of disruptive events, but also the processes that infrastructure systems undergo to maintain functionality following disruptions. This more comprehensive approach has been termed critical infrastructure resilience and has become a top-level strategic objective for DHS. In support of this objective, Sandia has formulated a unique assessment framework for evaluating the resilience of critical infrastructure and economic systems. This framework is the first of its kind that is flexible enough to consider all types of critical infrastructure systems while explicitly evaluating resources and costs of recovery.

The framework, illustrated in Figure 1, is composed of three primary components:

1. A newly formulated definition of system resilience that focuses on the system components that need to be considered for a resilience assessment;
2. A ***quantitative*** methodology for measuring system resilience; and
3. A ***qualitative*** methodology that can be used in place of, or to explain, quantitative results.

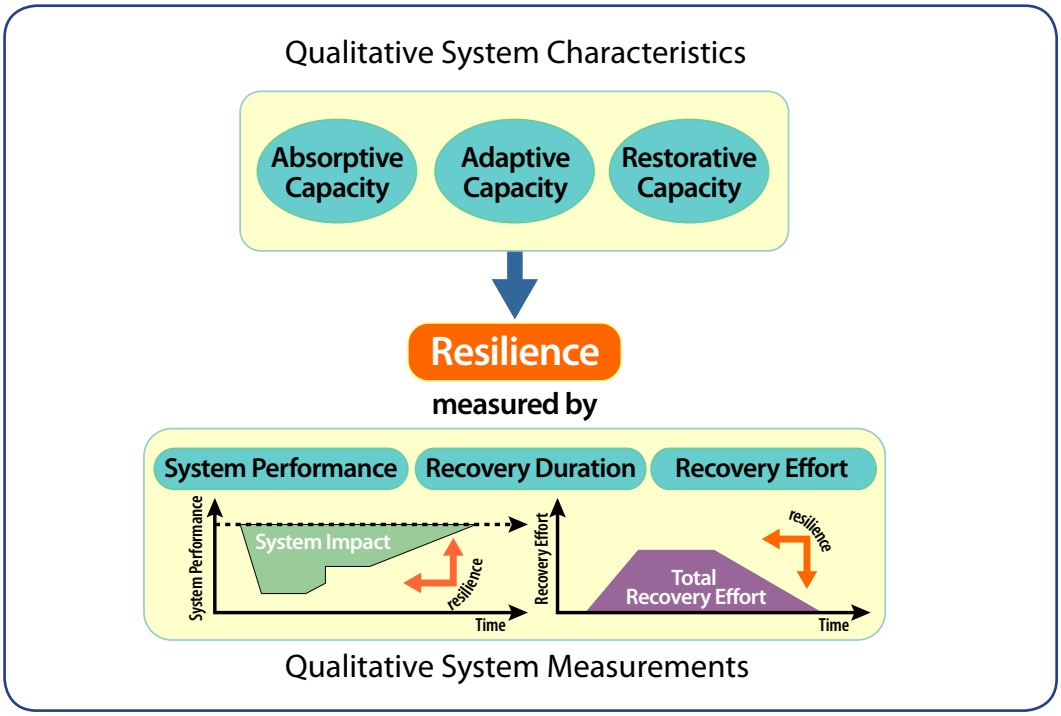

Figure 1: Sandia's resilience assessment framework combines qualitative system evaluations with quantitative measurements to provide a comprehensive resilience analysis, as shown in this conceptual rendering.

For more information:

Technical Contact:
Lillian Snyder
505-284-3378
lasnyde@sandia.gov

Science Matters Contact:
Alan Burns
505-844-9642
aburns@sandia.gov

Sandia National Laboratories

LDRD LABORATORY DIRECTED RESEARCH & DEVELOPMENT

The ***quantitative*** measurement methodology is founded in the mathematics of optimal control theory and evaluates both disruption impacts to infrastructure system performance and how resources are allocated to recover from a disruption. This portion of the resilience assessment framework can be used to select dynamic recovery strategies that enhance infrastructure resilience. Sandia is currently researching how the application of optimal control techniques can be used to develop optimal recovery strategies that maximize resilience and that may not have been previously identified by infrastructure system managers.

The ***qualitative*** methodology provides the analyst with a structured process for reviewing system features and structures that enhance or impede infrastructure resilience. Key system components are assigned to one of three resilience capacity categories: absorptive, adaptive, and restorative. This categorization provides the analyst insight into how the infrastructure system copes with a disruptive event by absorbing the initial impacts from the disruption, internally reorganizing and adapting to new system conditions, and/or receiving external assistance in recovering from the disruption and restoring functionality. The analyst can then use this insight to assess how to enhance infrastructure resilience. Together, the qualitative and quantitative components of the framework provide a comprehensive view of the resilience of the system along with the means for enhancing its resilience.

This framework has been used to assist DHS in preparing for large-scale disruptions to national critical infrastructure systems. The qualitative methodology has been implemented to assess the resilience of infrastructure systems in the Southern and Midwestern United States to a large earthquake in the New Madrid Seismic Zone. The entire framework is currently being applied to a set of chemical supply chains, with the goal of assessing the resilience of these supply chains to a number of natural and manmade disruption scenarios.

Integrated Cortical-Hippocampal Neural Architecture of Episodic Memory

New computational model improves fidelity to neurobiology

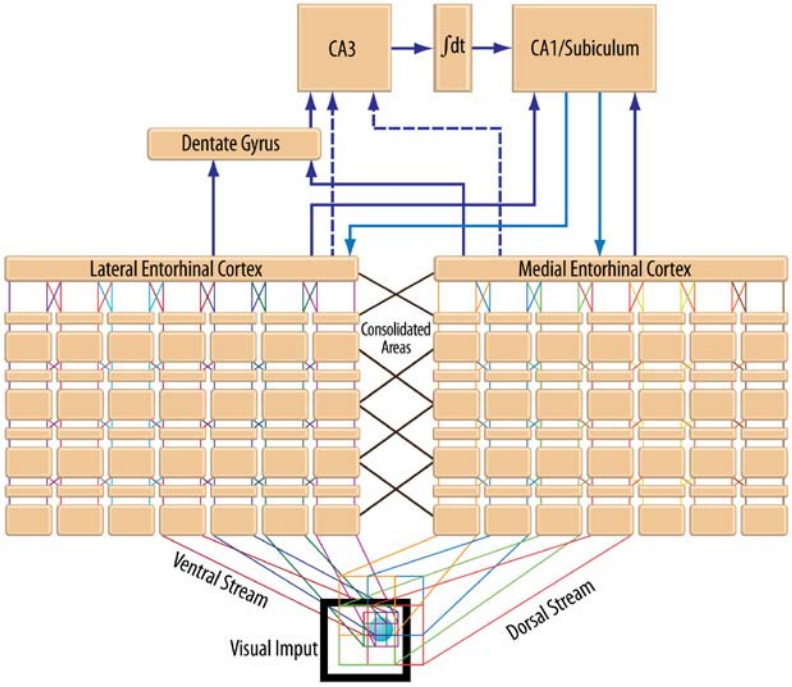

Figure 1: Simplified Sandia model.

For more information:

Technical Contact:
Michael Bernard
505-845-0815
mlberna@sandia.gov

Science Matters Contact:
Alan Burns
505-844-9642
aburns@sandia.gov

In cooperation with Boston University, the University of Illinois at Urbana-Champaign, and the University of New Mexico, Sandia is developing a neurologically plausible, artificial neural network architecture of episodic memory and recall, modeled after cortical-hippocampal structure and function.

The neural network architecture is based on research concerning multiple memory systems in the brain, and makes a distinction between declarative memory (for facts and events), and procedural or non-declarative memory (supporting the acquisition and expression of skills). Declarative memory is fundamentally relational, involving representations of the relations among the constituent elements of experience. This includes both episodic memory, constituting the binding together in memory of the who, what, where, and when of events, and semantic memory, involving binding in memory of information constituting the structured knowledge we acquire about the world.

Progressing from previous architecture versions in which the entire hippocampus was represented by a conjunctive grid, Sandia has instead developed individual modules to represent the primary regions of the hippocampus. This architecture is depicted in Figure 1. The main distinction between this approach and others is that it focuses more on the manipulation of memory relations rather than the encoding of specific events or neuronal activity. This is biologically plausible since it bases the architecture on estimates of the relative number of neurons and neuronal connections, but does not attempt to model the interaction between neurons individually. Building upon accepted

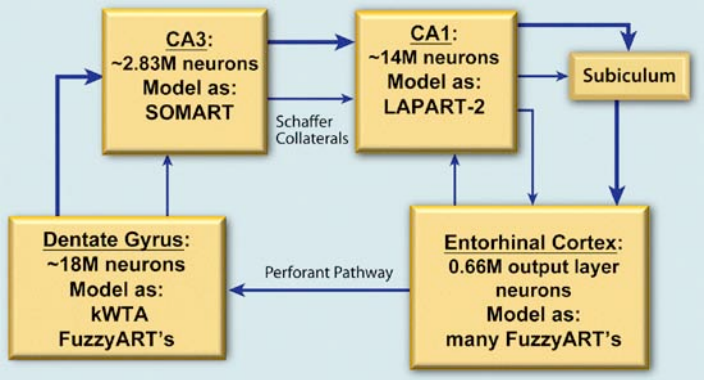

Figure 2: The relative number of human hippocampal neurons and the Sandia hippocampal loop representation.

hippocampus sub-region functionality, the researchers have implemented a computational architecture with conceptual processing based upon variants of Adaptive Resonance Theory (ART) for artificial neural networks. The pre-medial temporal lobe sensory cortex, and the entorhinal cortex (EC) are represented by layers of modified fuzzy-ART modules. The fuzzy-ART capabilities are extended by equipping these modules with the capability to encode temporal semantic data. Individually, these temporally integrated adaptive resonance theory (TIART) modules are capable of encoding categorical representations of their given input vectors over time. By combining layers of TIART modules, categories of categories may be formed to represent larger semantic concepts. In neuroanatomy, the EC receives multimodal sensory inputs. The model here simulates visual processing in which a dorsal stream containing contextual information and a ventral stream of focal information convene at the EC before entering the hippocampus.

Within the hippocampal representation in the model, each of the primary regions is represented by a different ART variant selected to achieve the particular functionality of the individual region. The relative size of each module is scaled in accordance with approximate human neuroanatomy. The particular module implementations as well as their respective size scaling may be seen in Figure 2.

The dentate gyrus (DG) receives the conjoined multimodal sensory signals from the EC. It performs pattern separation on this abundance of sensory information to produce sparse output activation, which ensures different semantic concepts are given unique encoding. This sparse output pattern from the DG serves as input to CA3. Functionally, CA3 assists with episodic binding through auto-association. In Sandia's model, this module is capable of mapping semantically similar inputs to proximate topological regions. In effect, related concepts are clustered together to help associate episodic memories. CA1 is involved in forming sequences of relations and connecting these episodic encodings back to the original sensory inputs from the EC. This ability to link sequences allows for temporal packaging of episodes. To handle the sequencing of associations, the researchers temporally integrate the inputs passed into the model's conjoined representation of CA1 and subiculum. A laterally primed adaptive resonance theory (LAPART) module represents the conjoined CA1 and subiculum regions. The LAPART module learns to associate CA3 encodings with the original unaltered EC inputs. This allows the LAPART module to complete the hippocampal loop and propagate temporal sequences back to EC and eventually to cortex for long term storage.

The progression of the computational model is driven by attempts to improve fidelity in relation to neurobiology. The approach has been to model neuroanatomy and in doing so, Sandia has demonstrated the ability to model elements of cognitive behavior such as familiarity and recognition. As a result of improving the hippocampal model the researchers are also able to create automatic associations of various semantic concepts (see Figure 3). In general, the artificial neural network computation model presented here processes sensory inputs and in effect is capable of exhibiting qualitative memory phenomena such as auto-association of episodic memory concepts.

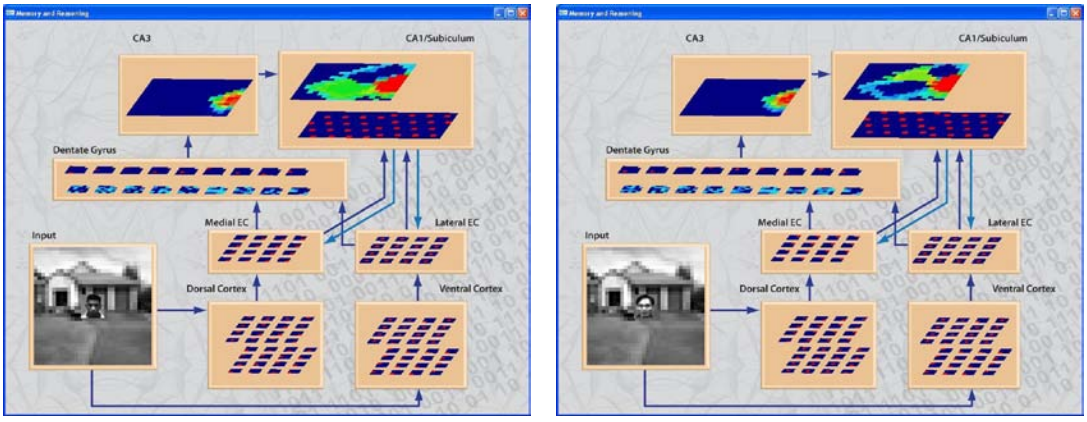

Figure 3: The current architecture can auto-associate and differentiate between different individuals with the same background.

$H_2S + 2Cu \rightarrow$

NNSA
National Nuclear Security Administration